Molecular Pathobiological Studies on Glutamate/Aspartate Transporter (GLAST) in Canine Red Cells

—Molecular Basis for Hereditary Deficiency of GLAST in Dogs —

イヌ赤血球グルタミン酸／アスパラギン酸輸送体（GLAST）に関する分子病態生理学的研究

—イヌにおける遺伝性 GLAST 欠損の分子機序—

Kota SATO

佐藤　耕太

2000

Contents

General Introduction

High-affinity Na^+-dependent glutamate transporters play important physiological roles in various mammalian tissues and cells. Several distinct glutamate transporters, GLAST[1], GLT-1, EAAC1, EAAT4, and EAAT5 have been cloned and their electrophysiological and pharmacological properties have been characterized (Storck *et al.*, 1992; Pines *et al.*, 1992; Kanai and Hediger, 1992; Fairman *et al.*, 1995; Arriza *et al.*, 1997). The transporters display 30-50% amino acid sequence similarity and almost identical hydrophobicity profiles, suggesting that their functional properties are based on similar structural traits. The uptake of glutamate is driven by the electrochemical gradients of Na^+, K^+, and H^+ or OH^- across the plasma membrane (Bouvier *et al.*, 1992) and is an electrogenic process (Roskoski *et al.*, 1981; Inaba and Maede, 1984; Bouvier *et al.*, 1992). Recent progress has demonstrated that these transporters function as Cl^- channels in addition to being co-transporter (Wadiche *et al.*, 1995). The Cl^- flux is activated by glutamate, but is not coupled to the transport of the substrates (Fairman *et al.*, 1995).

In the central nervous system, these transporters are highly differentially localized and participate in glutamate uptake into glial or neuronal cells to terminate excitatory neurotransmission (Nicholls and Attwell, 1990). In particular, glial transporters GLAST and GLT-1 play critical roles to maintain the extracellular glutamate concentration at the submicromolar level, thereby preventing accumulation of glutamate in the synaptic cleft, which causes overstimulation of the receptors and subsequent neurodegeneration. Dysfunction of glutamate transporters has been considered to be involved in the pathogenesis of neurodegenerative diseases such as

[1] Abbreviations used are: GLAST, glutamate/aspartate transporter; GLT-1, glutamate transporter-1; EAAC1, excitatory amino acid carrier 1; EAAT4 and -5, excitatory amino acid transporter 4 and -5, respectively.

amyotrophic lateral sclerosis (Lin *et al.*, 1998; Trotti *et al.*, 1998), Alzheimer's disease, trauma, and ischemia (Trotti *et al.*, 1998). Selective depletion of glutamate transporters, particularly glial transporters GLAST and GLT-1, by chronic administration of antisense oligonucleotides in living rats led to the appearance of neurological symptoms, including seizures and progressive limb weakness (Rothstein *et al.*, 1996). In peripheral tissues, glutamate transporters are believed to have pivotal functions in epithelial transport and absorption of acidic amino acids, glutamate, and aspartate (Schneider *et al.*, 1980; Rajendran *et al.*, 1987; Heinz *et al.*, 1988), and in modulation of glutathione synthesis (Deneke *et al.*, 1987). EAAC1 is presumed to be a transporter in the epithelia of the intestine and kidney, because its transcripts were identified in those peripheral tissues as well as in neurons (Kanai and Hediger, 1992). However, physiological and pathological functions of other transporter isoforms in peripheral tissues have not been well characterized.

I have been interested in the structure, function, and regulation of expression of the red cell glutamate transporter in dogs. Canine red cells possess a high affinity Na^+- and K^+-dependent L-glutamate and L-aspartate transport system (Inaba and Maede, 1984), in contrast to the fact that most mammalian red cells are impermeable to these acidic amino acids (Young and Ellory, 1977). Dogs usually have red cells with low K^+ and high Na^+ concentrations (LK red cells) because they lose red cell Na,K-ATPase during reticulocyte maturation (Maede and Inaba, 1985; Inaba and Maede, 1986). However, some Japanese Shiba and mongrel dogs have HK red cells with high Na,K-ATPase activity, resulting in high K^+ and low Na^+ concentrations, and this HK phenotype is inherited in an autosomal recessive manner (Maede *et al.*, 1983). HK red cells show accelerated Na^+/K^+-dependent glutamate/aspartate uptake due to an increased concentration gradient of Na^+ and K^+ across the plasma membrane, leading

to marked accumulations of intracellular glutamate, aspartate, and glutamine (Maede *et al.*, 1983; Inaba and Maede, 1984). The increased concentration of glutamate further results in an elevated level of reduced glutathione and affects the redox state and protection against oxidative stress of the red cell (Maede *et al.*, 1989). Interestingly, these breeds also include dogs characterized by reduced (Fujise *et al.*, 1993) and nondetectable (K. Sato, M., Inaba, and Y. Maede, unpublished observation, Oct. 1991) red cell glutamate transport, generating variant HK cells without accumulation of glutathione. Their red cells were readily accessible to oxidants such as acetylphenyl hydrazine and generated Heinz bodies much more than normal HK cells or even LK red cells did (K. Sato, M. Inaba, and K. Kagota, unpublished observation, Apr. 1999). Such a hereditary defect of the glutamate transporter in mammals has never been described, although several pathological studies on mice lacking glutamate transporters due to gene disruption have been reported (Tanaka *et al.*, 1997; Harada *et al.*, 1998). The observations in the dogs suggested that the functions of the glutamate transporters contributed to protect cellular contents from oxidative damage in peripheral tissues. Moreover, recent studies have suggested a direct link between oxidation and neurodegeneration based on the vulnerability to biological oxidants and possible involvement of an SH-based redox regulatory mechanism of glutamate transporters including GLAST and GLT-1 (Trotti *et al.*, 1998). Defining the molecular basis that underlies the transport deficiency in canine red cells may facilitate our understanding of the regulatory mechanisms for expression of, and the physiological and pathological roles of the glutamate transporter in various tissues, including the brain. The purpose of the present study is to precisely define the glutamate transporter in canine red cells, thereby clarifying the underlying cause for the hereditary deficiency of the transport. In Chapter 1, stoichiometric and pharmacologic properties of Na^+-dependent glutamate transport in canine red cells were investigated extensively. In Chapter 2, canine red cell transporter was identified by PCR-based cloning of several different transporter subtypes, functional analysis of the isolated clones in *Xenopus* oocyte expression

system, and immunological identification. Based on the findings on molecular features of the red cell glutamate transporter, molecular basis for the inherited defects of the transport found in a family of dogs that led to decreased level of red cell glutathione and a high susceptibility to oxidative stress of red cells was investigated in Chapter 3.

Chapter 1

Characterization of Glutamate Transport in Canine Red Cells

Introduction

A high affinity glutamate transport system, designated as system X^-_{AG}, has been found in a variety of tissues and cells (Kanner and Sharon, 1978; Sips *et al.*, 1982; Rajendran *et al.*, 1987; Heinz *et al.*, 1988; Hoeltzli *et al.*, 1990; Nicholls and Attwell, 1990; Kanner *et al.*, 1993). The transporter plays important physiological roles such as termination of neurotransmission in the central nervous system (Nicholls and Attwell, 1990) and absorption of acidic amino acids in small intestine (Rajendran *et al.*, 1987) and kidney (Heinz *et al.*, 1988). Five different Na^+-dependent glutamate transporters have been cloned in brain (Storck *et al.*, 1992; Pines *et al.*, 1992; Fairman *et al.*, 1995) , intestine (Kanai and Hediger, 1992) or retina (Arriza *et al.*, 1997). Although they are very similar in primary structure, their tissue distributions are quite different from each other (Storck *et al.*, 1992; Pines *et al.*, 1992; Kanai and Hediger, 1992; Fairman *et al.*, 1995; Arriza *et al.*, 1997).

Canine red cells possess an Na^+-dependent electrogenic transport system for L-glutamate and L-aspartate (Inaba and Maede, 1984) in contrast to that most mammalian red cells are impermeable to these acidic amino acids (Young and Ellory, 1977). Red cells with high K^+ and low Na^+ concentrations (HK cells) incorporate these amino acids more actively than LK cells with low K^+ and high Na^+ concentrations because of the increased Na^+ gradient across the plasma membrane, resulting in accumulation of glutamate, and, consequently, in an increased concentration of glutathione (Maede *et al.*, 1983). Therefore, in canine red cells, the transporter serves to supply glutamate as the substrate for production of glutathione to protect the cells from oxidative stress (Maede *et al.*, 1983).

These transporters showed similar characteristics in their Na^+-dependence, affinities to the substrates and electrogenicity (Inaba and Maede, 1984). However, the stoichiometry of ion coupling, that is, what kind of and how many ions are involved in the electrogenic pathway, has not been precisely determined. Bouvier *et al.* (1992)

demonstrated a unique complicated stoichiometry of glutamate transport in salamander retinal glial cells that was coupled to OH^- (or HCO_3^-) counter transport in addition to cotransport of two Na^+ ions and counter transport of one K^+ ion. The purpose of the study in Chapter 1 was to evaluate if such complicated stoichiometry exists in the mammalian glutamate transport system and to elucidate which subtype of brain transporters displays characteristics of glutamate transport in canine red cells. Here, the ionic dependence of cations (Na^+ and K^+) and various anions, and substrate specificity of canine red cell glutamate transport system were investigated.

Materials and Methods

Chemicals The sources of chemicals were as follows. L-[3,4-^{3}H]Glutamic acid (49 Ci/mmol) was from NEN Life Science Products (Boston, MA, U.S.A.). L-Glutamic acid, D-glutamic acid, L-aspartic acid, D-aspartic acid and acetazolamide from Wako Pure Chemical Industries (Osaka, Japan), *threo*-3-hydroxyaspartate from Tocris Neuramine (Bristol, United Kingdom), dihydrokainate (2-carboxy-4-isopropyl-3-pyrrolidine acetic acid, DHK), DL-α-aminoadipic acid, L-cysteinesulfinic acid, phenylmethylsulfonyl fluoride (PMSF) and valinomycin from Sigma (St. Louis, MO, U.S.A.), and 4,4'-diisothiocyanostilbene-2-2'-disulfonic acid (DIDS) from Dojin Laboratories (Kumamoto, Japan). All other chemicals were of the purest grade available.

Preparation of red cell suspension Preparation of red cell suspension was carried out as previously described with some modification (Inaba and Maede, 1984). Heparinized venous blood from HK or LK dogs was washed three times at 4°C with an incubation medium containing 150 mM NaCl, 1 mM $MgCl_2$, 5 mM D-glucose, 0.1% (w/v) bovine serum albumin (BSA) and 10 mM 3-(*N*-morpholino)propanesulfonic acid (Mops)/Tris (pH 7.4). When Na^+ dependence and substrate specificities were examined, the incubation medium also contained 5 mM KCl. The washed cells were resuspended in the same medium to yield a hematocrit value of 20 %.

Preparation of the resealed ghosts Resealed ghosts were prepared according to the procedure of Klonk and Deuticke (Klonk and Deuticke, 1992). Heparinized venous blood from LK dogs was centrifuged at 1,000 x g for 5 min and plasma and buffy coat cells were removed by aspiration. The cells were washed three times with Na^+-K^+ free phosphate buffer (150 mM choline chloride, 1 mM $MgCl_2$, and 10 mM orthophosphoric acid/ Tris (pH7.4)) at 4°C. The last centrifugation was done at 2,000 x g for 10 min and supernatant was sufficiently removed. One volume of packed cells was lysed in 40 volumes of the hypotonic buffer (5 mM orthophosphoric acid/Tris

(pH7.4), 1 mM $MgCl_2$, 0.8 mM PMSF) with stirring for 10 min on ice. Unsealed ghosts were pelleted by centrifugations at 15,000 x g for 20 min. One volume of unsealed ghosts were diluted with an equal volume of hypotonic buffer followed by the addition of 0.5 volumes of 5x reconstitution buffer containing 750 mM KCl or choline chloride, 100 mM Mops/Tris (pH7.4) with gentle stirring on ice for 10 min. The internal K^+ concentration was changed by a combination of the reconstitution buffers (see figure legends for details). This mixture was incubated for 45 min at 37°C and centrifuged for 5 min at 15,000 x g. The supernatant was thoroughly removed and resealed ghosts were obtained as pink pellets.

Measurement of L-glutamate transport L-Glutamate uptake was measured as previously described (Inaba and Maede, 1984). Briefly, 100 µl of the incubation medium containing 1-5 µCi/ml L-[^{3}H] glutamate was added to 100 µl of the red cell suspension and incubated at 37°C for the indicated periods. Structural analogues of L-glutamate were added at 25 µM, when present. Incubation was stopped by the addition of 1 ml of ice-cold incubation medium and the cells were washed with the same buffer by repeated centrifugation (15,000 x g, 10 sec). After the final wash, cells were lysed by the addition of 200 µl of 0.5% (v/v) Triton X-100 followed by the addition of 200 µl of 5% (w/v) trichloroacetic acid and centrifuged (15,000 x g, 3 min). The resulting 200-µl supernatants were counted for radioactivity using the solid scintillant Ready Cap (Beckman, Fullerton, CA, U.S.A.). The results were expressed as nmoles/ml cells.

When the internal anions were replaced, 100 µl of HK cell suspension was prepared as described above. The cells were washed three times with the medium containing 150 mM NaX (X = Cl, Br, F, I) or 25 mM $NaHCO_3$/5% CO_2+125 mM NaCl, 5 mM KCl, 1 mM $MgCl_2$, 5 mM D-glucose, 0.1% BSA, 10 mM Mops/Tris (pH7.4), at 4°C and placed at room temperature (22°C) for 5 min to load the cells with each anion via an anion exchanger (band 3). Fifty microliters of the supernatant were removed from the cell suspensions after rapid centrifugation (15,000 x g, 10 sec) and

resuspended cells were preincubated at 37°C for 1 min. Uptake of L-glutamate was measured at 37°C for 1 min by the addition of 250 µl of medium containing 150 mM Na gluconate, 5 mM KCl, 1 mM $MgCl_2$, 5 mM D-glucose, 0.1% BSA, 10 mM Mops/Tris (pH7.4), 6 µM L-[^{3}H]glutamate, 6 µM valinomycin and 12 µM DIDS. Movement of anions was diminished by DIDS, which is specific inhibitor for band 3 (Cabantchik *et al.*, 1978). Valionomycin was also added to abolish the effect of membrane potential, which is altered when anion exchange is inhibited (Payne *et al.*, 1990). Thus, 125 mM Na gluconate, 25 mM Na salts of loaded anions, 5 µM L-[^{3}H]glutamate and valinomycin, and 10 µM DIDS were present outside the cells in this system. To assess the effect of external anion substitution, the cells were suspended in the medium containing 150 mM NaCl, 5 mM KCl, 1 mM $MgCl_2$, 5 mM D-glucose, 0.1% BSA, 10 mM Mops/Tris (pH7.4), with an Hct value of 20%. The L-glutamate uptake was measured at 37°C for 1 min in medium containing 150 mM NaX (X = Cl, Br, F, I) or 25 mM $NaHCO_3$/5% CO_2+125 mM NaCl using the same procedure as internal anion substitution.

When L-glutamate uptake in resealed ghosts was measured, 190 µl of medium containing 150 mM NaCl, 20 mM Mops/Tris (pH7.4), and 1-5 µCi/ml L-glutamate was added to 10 µl of resealed ghosts. After the incubation, the resealed ghosts were washed with the ice-cold medium three times by centrifugation at 15,000 x g for 30 sec. A hundred microliter each of 0.5% Triton X-100 and 5% trichloroacetic acid were added and centrifuged and the resulting supernatant was used for counting radioactivity. The results were expressed as nmoles/mg protein. The protein contents of the resealed ghosts were determined by the method of Bradford (1976) with bovine serum albumin as the standard. To determine the membrane protein contents of the resealed ghosts, hemoglobin-depleted ghosts were prepared from the resealed ones by hypotonic lysis and washing (Inaba and Maede, 1986).

The efflux of L-glutamate was measured in the LK cells preloaded with 40 nM (2

μCi/ml) L-[^{3}H] glutamate at 37°C for 30 min in medium containing 150 mM NaCl, 5 mM KCl, 1 mM $MgCl_2$, 5 mM D-glucose, 0.1% BSA and 10 mM Mops/Tris (pH7.4). The loaded cells were washed three times with the ice-cold efflux medium containing NaCl and/or KCl (NaCl + KCl = 150 mM), 5 mM KCl, 1 mM $MgCl_2$, 5 mM D-glucose, 0.1% BSA, 10 mM Mops/Tris (pH7.4), Fifty-microliters of the cell suspension (Hct = 20%) were added to 1 ml of the same efflux medium. After incubation for the indicated period at 37°C, the radioactivity of L-[^{3}H]glutamate retained in the cells was determined as described above. The efflux was expressed as a percentage of the retained radioactivity at time 0.

Results

The ionic dependence of L-glutamate transport in canine red cells was investigated in intact cells and resealed ghosts. The dependence on external Na^+ was determined in LK cells to minimize the association of the K^+ gradient (Fig. 1). The sigmoidal dependence on the Na^+ concentration suggested that multiple Na^+ ions were involved in the transport process. Analysis by Hill's equation showed a Hill coefficient of 2.01 and half activation at 71 mM $[Na^+]_{out}$ (Fig. 1, *inset*), indicating that two Na^+ ions were involved in the transport process.

Fig. 2 shows that high-affinity Na^+-dependent L-glutamate transport was reconstituted in the resealed ghosts that contained K^+ as the internal cation. However, when internal K^+ was replaced by choline, L-glutamate uptake was totally abolished (Fig. 2). Thus, it was demonstrated that not only external Na^+ but also internal K^+ was required for the L-glutamate transport, as demonstrated for the transporter in rat brain (Kanner and Sharon, 1978; Pines *et al.*, 1992). We surveyed the dependence of the uptake on the internal K^+ concentration and K^+ gradient in resealed ghosts (Fig. 3). External K^+ inhibited L-glutamate transport according to its concentration, suggesting that the outward gradient of K^+ gradient facilitated the uptake. This is consistent with the model in which the efflux of K^+ was coupled to L-glutamate influx. Kinetic analysis showed that the dependence on internal K^+ fit to a simple Michaelis-Menten equation, equivalent to Hill's model with a Hill coefficient of 1.0, with a K_m value of 23 mM and a V_{max} of 0.41 nmoles/mg protein per 10 min under conditions in which $[Na^+]_{out}$ = 100 mM, $[K^+]_{out}$ = 0 and [L-glutamate]$_{out}$ = 5 μM (Fig. 3A and 3B). The first-order dependence of glutamate uptake suggested that one K^+ ion was involved in the transport process.

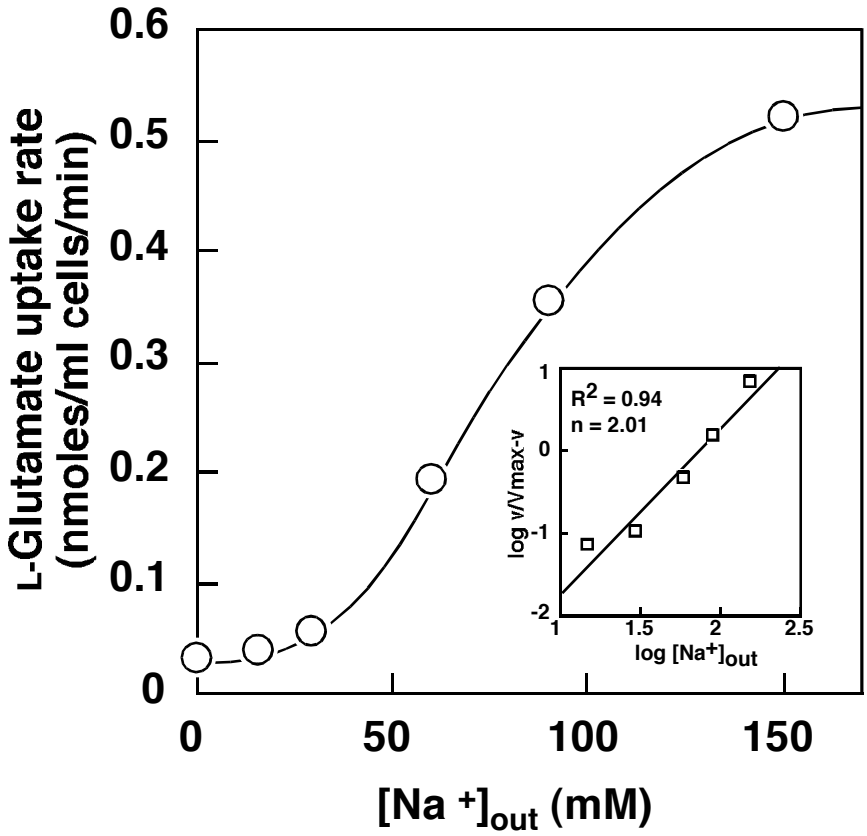

Figure 1. The dependence on the external Na^+ of L-glutamate transport in canine red cells. Uptake of 5 μM L-[^{3}H]glutamate (1 μCi/ml) was measured at 37°C for 2 min in medium containing x mM NaCl (x = 0-150) and 150-x mM choline chloride. Data were expressed as mean values of experiments in duplicate. Linear transformation of data expressed as the Hill's equation is shown in the inset.

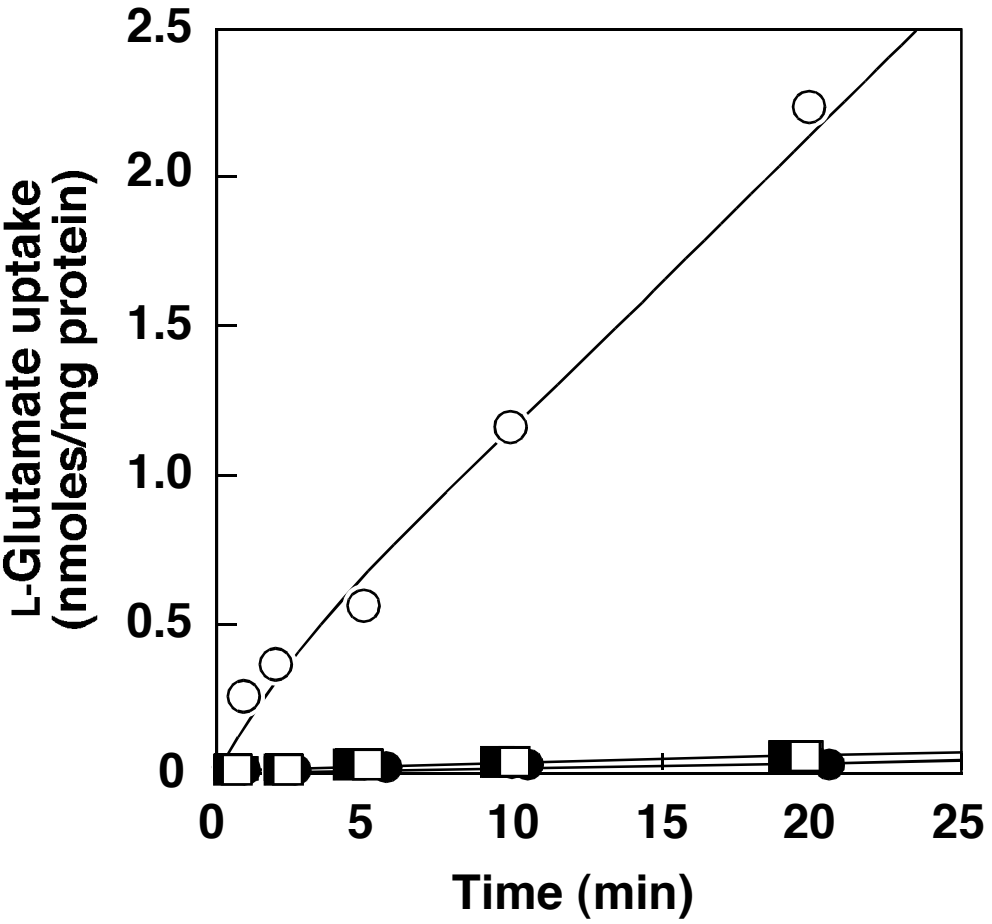

Figure 2. The requirement of Na^+ and K^+ in L-glutamate transport. Resealed ghosts were loaded with 150 mM KCl (○, ●) or 150 mM choline chloride (□, ■). Uptake of 5 μM L-[^{3}H]glutamate (2 μCi/ml) was measured at 37°C for the indicated periods in medium containing 150 mM NaCl (○, □) or choline chloride (●, ■). Data are expressed as mean values of experiments in duplicate.

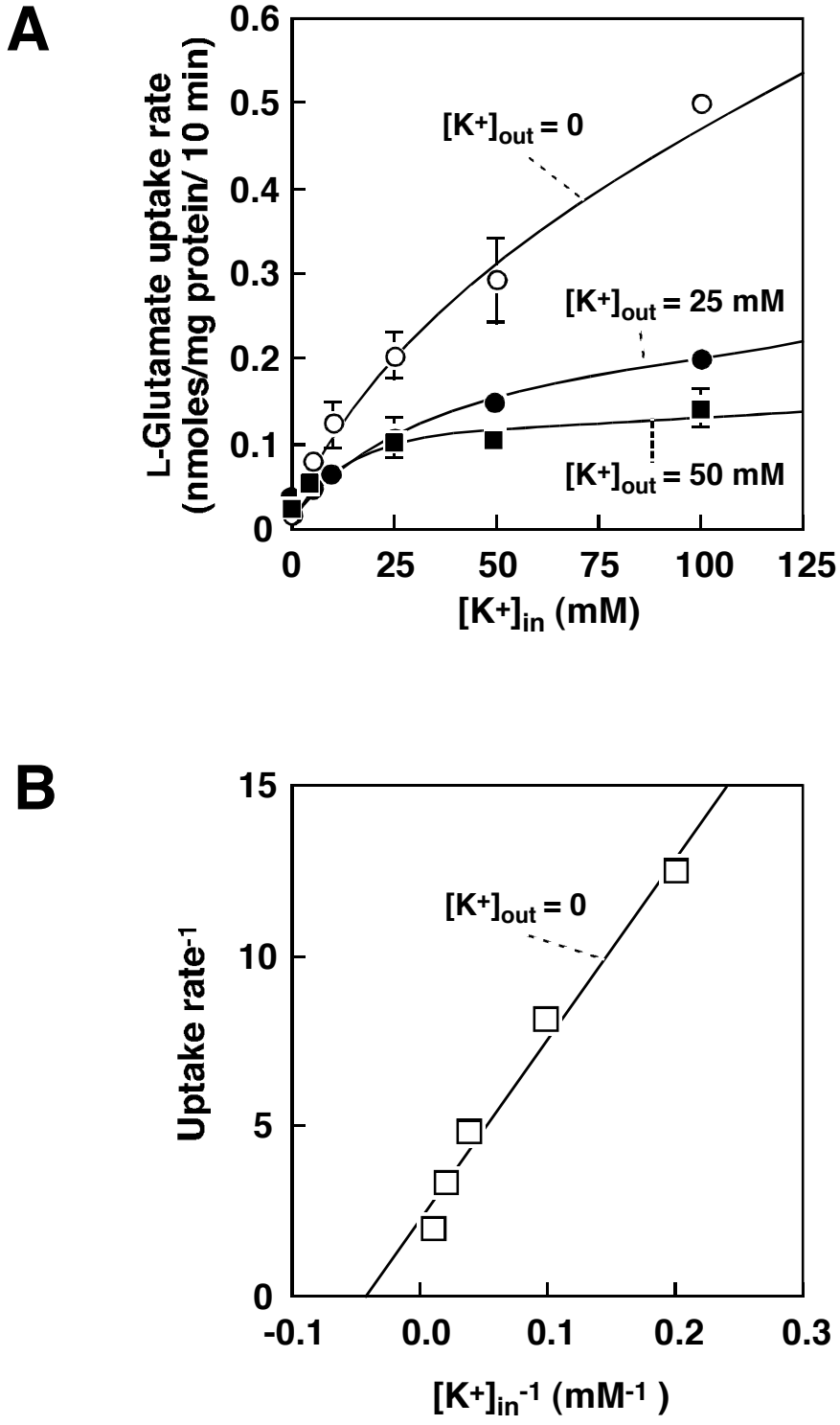

Figure 3. The dependence on the internal K+ of L-glutamate transport in resealed ghosts. Resealed ghosts were loaded with x mM KCl (x = 0-100) and 150-x mM choline chloride. Uptake of 5 μM L-[^{3}H]glutamate (2 μCi/ml) (A) was measured at 37°C for 10 min in medium containing 100 mM NaCl, 0 (○) or 25 mM (●) or 50 mM (■) KCl (50 mM, 25 mM and 0 choline chloride were added, respectively). Data are expressed as mean ± S.D. of experiments in triplicate and linearized by Lineweaver-Burk plot (B) with the data of $[K+]_{out} = 0$.

The dependence on the external L-glutamate concentration was also described by a Michaelis-Menten equation with a K_m value of 7.2 μM and a V_{max} of 1.89 nmoles/mg protein per 10 min ($[Na^+]_{out}$ = 100 mM, $[K^+]_{out}$ = 0). This first-order dependence suggestedthat one L-glutamate was associated with the transport cycle (Fig. 4). When the external K^+ concentration was raised to 50 mM ($[Na^+]_{out}$ = 100 mM), the V_{max} value decreased to 0.57 nmoles/ml cells per 10 min without a significant change of the K_m value (12.1 μM), indicating that the inhibition by external K^+ (Fig. 3 and Fig. 4) was not caused by a change of affinity to L-glutamate.

Fig. 5 shows the efflux of L-glutamate from canine red cells. Approximately 90% of L-glutamate within the cells was retained even after 2 h incubation when the inward Na^+ and outward K^+ gradients were present ($[Na^+]_{out}$ = 150 mM and $[K^+]_{out}$ = 0). However, retained L-glutamate was markedly decreased when the extracellular concentrations of Na^+ and K^+ were changed to 100 mM or less and 50 mM or more, respectively, which were sufficient to reverse the gradient directions of these cations in LK cells (Maede *et al.*, 1983). These results suggested that L-glutamate can be transported by the transporter in the opposite direction using reverse gradients of Na^+ and K^+ as the driving forces. This could be the cause of the apparent inhibition of the transport by external K^+ described above.

These results showed that Na^+ and K^+ are completely coupled to L-glutamate transport, and that two Na^+ and a K^+ are involved in each transport cycle. This stoichiometry is electroneutral while the transport process is considered to be electrogenic in intact cells (Inaba and Maede, 1984) and resealed ghosts. Therefore, the effect was examined for replacement of intracellular or extracellular Cl^- by several other anions. Extracellular HCO_3^- (added as 15 mM $NaHCO_3$/5% CO_2) increased the uptake by 20% as shown in Fig. 6. This effect of extracellular HCO_3^- disappeared in the presence of acetazolamide, a carbonic anhydrase inhibitor, although acetazolamide itself did not change the uptake in the Cl^- medium (Fig. 6). When the uptake was measured in the presence of DIDS

and valinomycin, some halides increased the L-glutamate uptake in the order $F^- > Br^- > Cl^- \geq I^-$ despite their intra- and extracellular distribution (Fig. 7). Under the same condition, the cells loaded with 25 mM HCO_3^- showed an increase in transport of L-glutamate by 55% that was as intensive as F^--loaded cells, whereas the addition of 25 mM HCO_3^- outside the cells did not affect the uptake. These results demonstrated that HCO_3^- accumulated inside the red cells facilitated L-glutamate transport.

Several structural derivatives of L-glutamate were tested for their inhibitory effects on glutamate uptake into red cells. Cross-inhibition analysis revealed that the canine red cell L-glutamate transport system was highly sensitive to *threo*-3-hydroxyaspartate and L-cysteinesulfinate as well as to L- and D-aspartate (Fig. 8). *threo*-3-Hydroxyaspartate is a potent inhibitor of the transporter in rat brain (Storck *et al.*, 1992) and L-cysteinesulfinate is another candidate for physiological substrate (Recasens *et al.*, 1982). In contrast, the use of dihydrokainate and DL-α-aminoadipate, both of which suppressed glial uptake by 70-90% (Pines *et al.*, 1992), resulted in no obvious inhibition in the red cells. Dihydrokainate and L-cysteine poorly inhibited the glutamate transport in canine red cells.

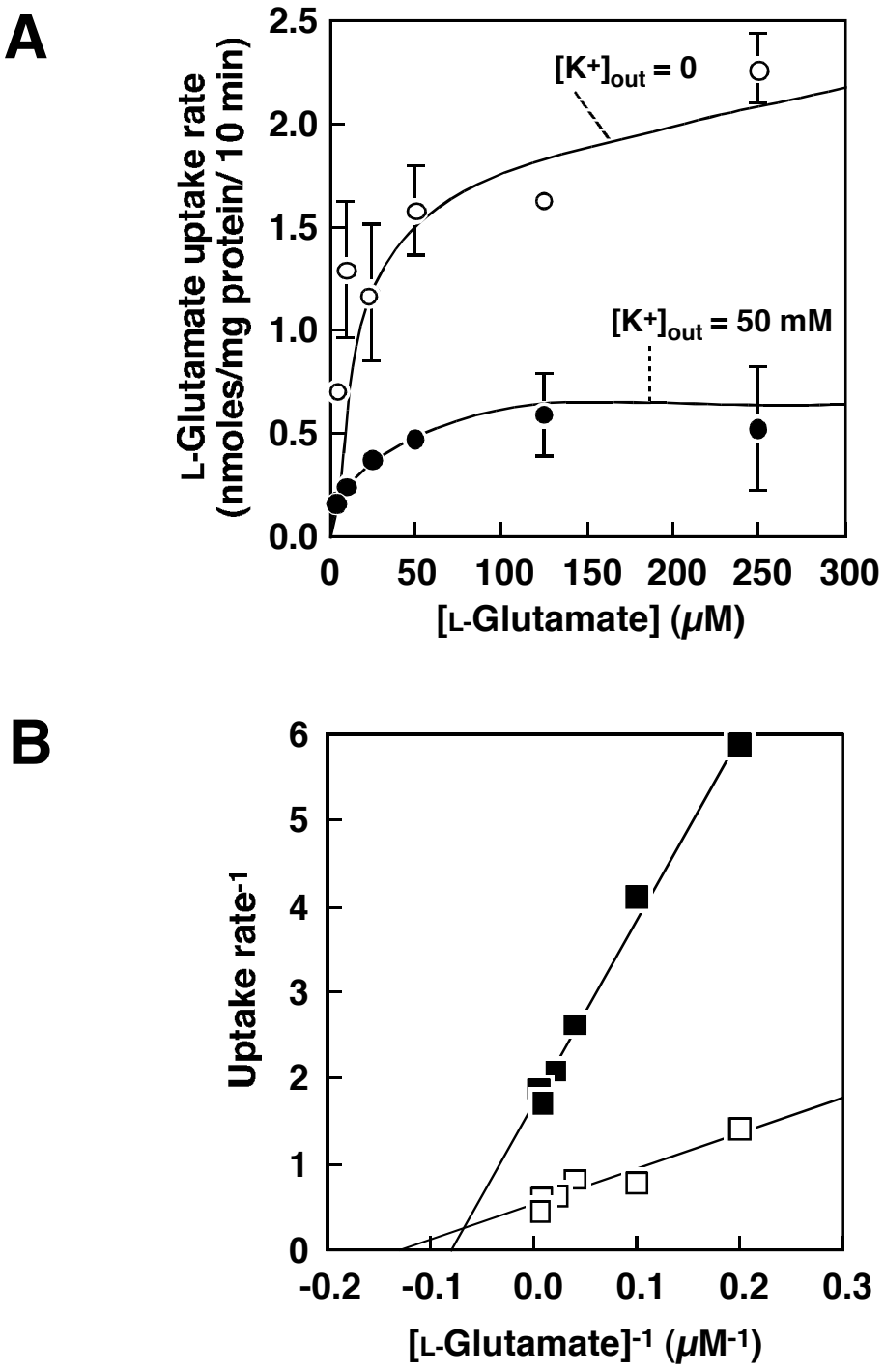

Figure 4. Effect of the external K^+ and L-glutamate concentration on the uptake of L-glutamate in resealed ghosts. Resealed ghosts were loaded with 100 mM KCl, 50 mM choline chloride. Uptake of L-[^{3}H]glutamate (1-5 μCi/ml) by the resealed ghosts (A) was measured at 37°C for 10 min in medium containing 100 mM NaCl, 50 mM KCl (●)or choline chloride (○) and various concentration of L-glutamate. Data are expressed as mean ± S.D. of determinations in triplicate and linearized by Lineweaver-Burk plot (B).

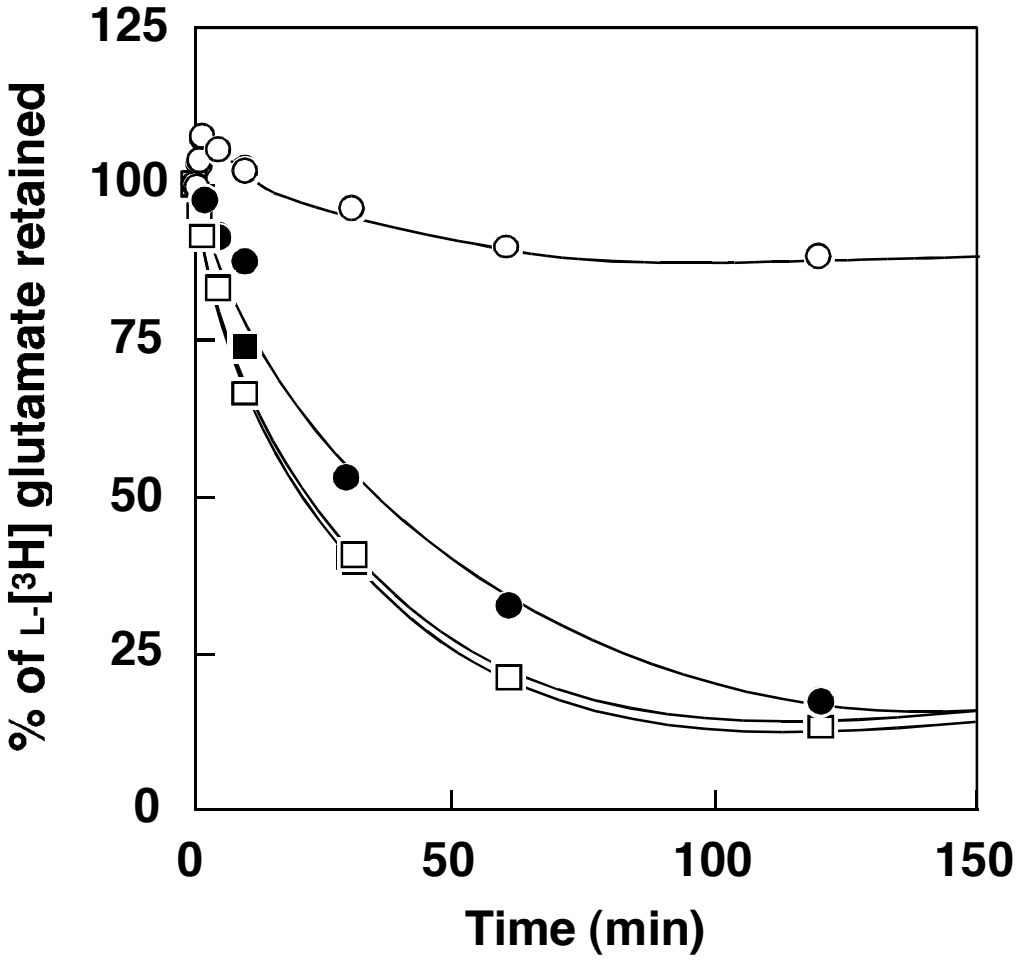

Figure 5. The efflux of L-glutamate from canine red cells. LK red cells were loaded with 40 nM L-[^{3}H]glutamate (2 μCi/ml) in medium containing 150 mM NaCl at 37°C for 30 min. Percentage of the retained L-[^{3}H]glutamate were measured after incubation of the L-[^{3}H]glutamate loaded cells for the indicated periods at 37°C in medium containing 150 mM NaCl (○), 100 mM NaCl + 50 mM KCl (●), 50 mM NaCl + 100 mM KCl (□) and 150 mM KCl (■). Data are expressed as mean ± S.D. of determinations in duplicate.

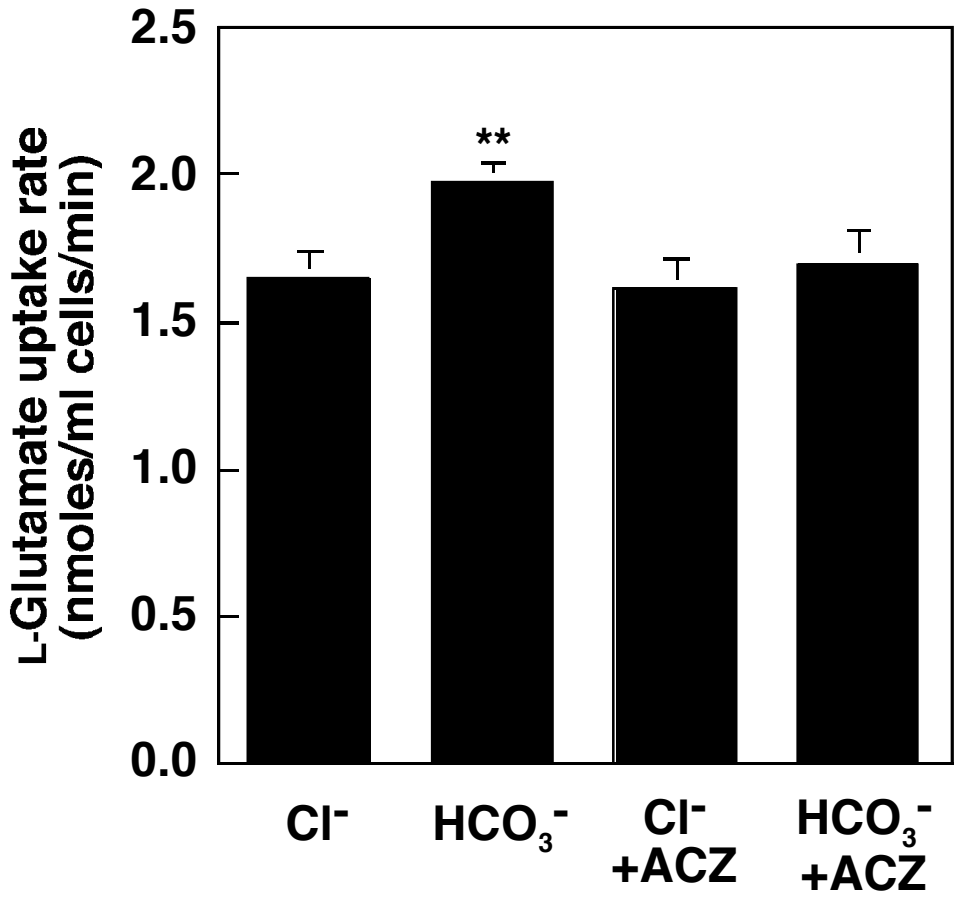

Figure 6. Effect of HCO_3^-/CO_2 buffer on L-glutamate transport in canine red cells. Uptake of 5 μM L-[^{3}H]glutamate (1 μCi/ml) was measured at 37°C for 1 min in medium containing 150 mM NaCl or 135 mM NaCl + 15 mM $NaHCO_3$/5% CO_2 with or without 1 mM acetazolamide (ACZ). Data are expressed as mean ± S.D. (n=7, $^{**}P < 0.01$, *t*-test compared with the uptake value in Cl^- without ACZ).

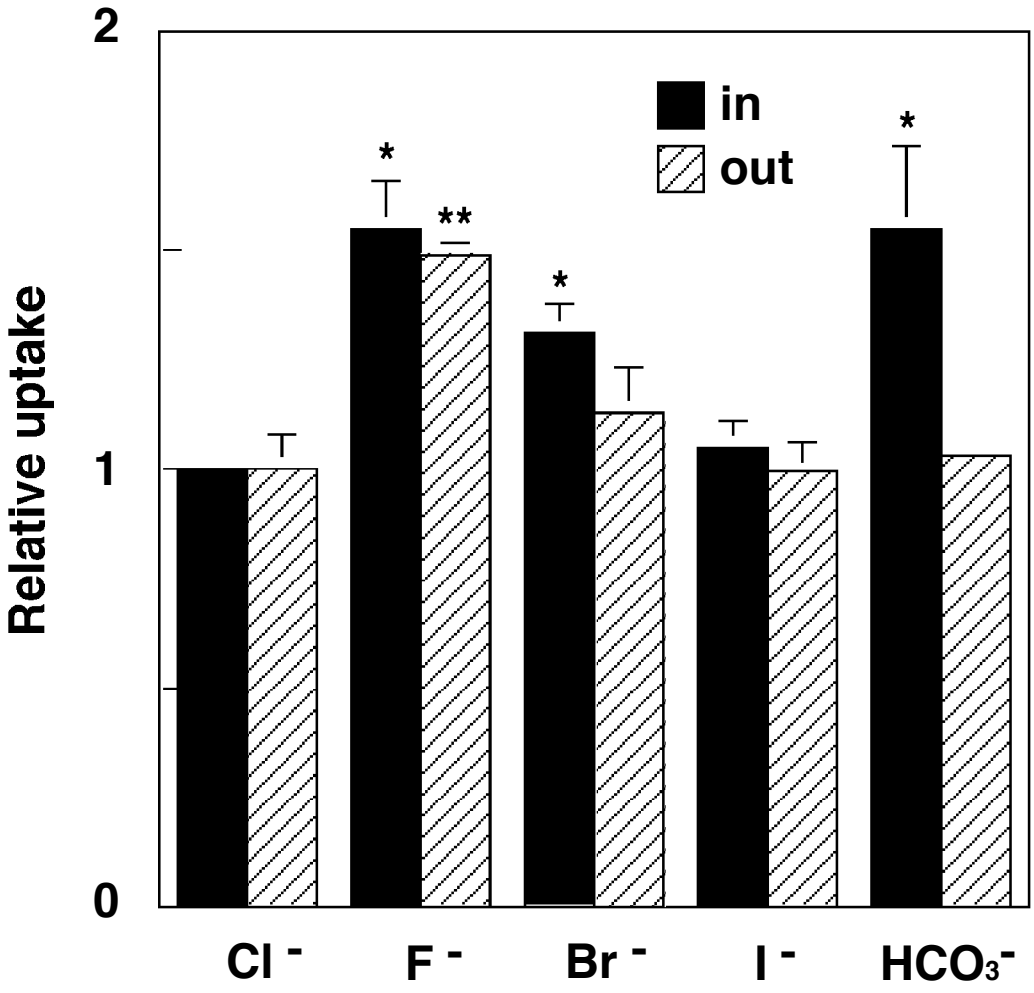

Figure 7. Effects of diverse anions on L-glutamate transport in canine red cells. HK red cells were loaded with diverse anions by incubation at 22°C for 5 min in medium containing 150 mM NaX (X = Cl, F, Br, I) or 125 mM NaCl+25 mM $NaHCO_3$/5% CO_2. Uptake of 5 μM L-[^{3}H]glutamate (1 μCi/ml) was measured at 37°C for 1 min in medium containing 150 mM Na gluconate in the presence of 10 μM DIDS and 5 μM valinomycin. Data are expressed as mean±S.D. of the relative uptake (Cl^- = 1.0, n = 3, *P < 0.05, **P < 0.01, t-test compared with the uptake value in Cl^-).

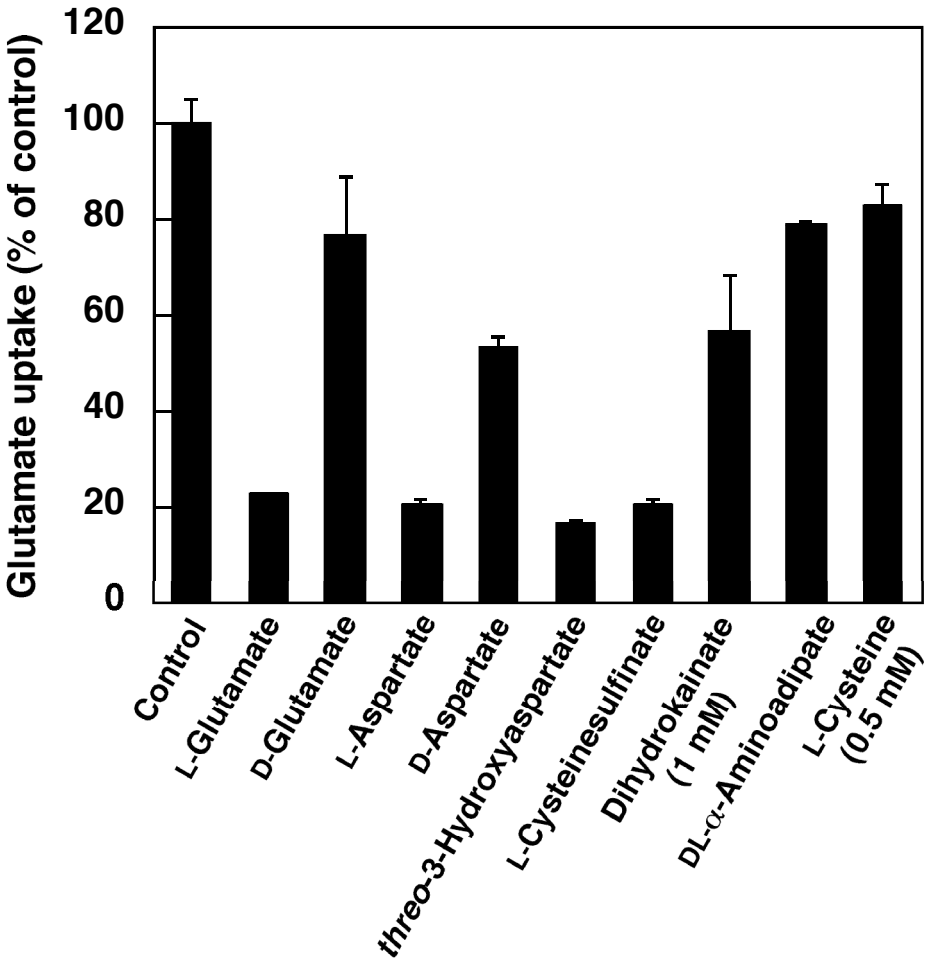

Figure 8. Cross-inhibition of L-glutamate transport in canine red cells by structural analogues. Uptake of 5 μM L-[^{3}H]glutamate (1 μCi/ml) was measured with HK cells at 37°C for 5 min in medium containing 25 μM of each analogue unless otherwise stated. Data are expressed as mean ± S.D. of determination in triplicate.

Discussion

This study demonstrated that high-affinity L-glutamate transport in canine red cells is coupled to cotransport of two Na^+ ions and countertransport of one K^+ ion (Figs. 1 and 3). Since the transport process is electrogenic as reported previously (Inaba and Maede, 1984), the stoichiometry should require additional movement of other cation(s) such as H^+ or anion(s). Bouvier *et al.* (1992) have proposed, based on several electrophysiological investigations in salamander retinal glial cells (Barbour *et al.*, 1988), the stoichiometry involving cotransport of two Na^+ ions and countertransport of one K^+ ion and one pH changing anion for one glutamate. According to the anion involved in the transport of L-glutamate, they suggested that OH^- is the main anion transported and that occasionally HCO_3^- is transported *in vivo* because they did not observe a significant decrease of pH due to L-glutamate movement across the membrane of the cells in which carbonic anhydrase was blocked (Bouvier *et al.*, 1992). Direct measurement of uptake in the present study demonstrated that the transport was enhanced by HCO_3^- at physiological concentrations (15-25 mM $NaHCO_3$/5% CO_2). This increase was diminished by acetazolamide, a potent inhibitor of carbonic anhydrase, suggesting a stimulating effect of HCO_3^- accumulated within the cells (Fig. 6). The effect of HCO_3^- was more evident when the major transport system for HCO_3^- in red cells, band 3 (Cabantchik *et al.*, 1978), was blocked with DIDS after partial substitution of HCO_3^- for internal anions (Fig. 7). These results indicated that L-glutamate transport in canine red cells was stimulated in the presence of internal HCO_3^- as the substrate anion. However, L-glutamate uptake was not disturbed by HCO_3^- deprivation in resealed ghosts (Figs. 3 and 4) or in red cells suspended in medium degassed and equilibrated with N_2 (data not shown), indicating that a major basal fraction of the L-glutamate uptake was linked to movement of anions other than HCO_3^-, such as OH^-. It is most likely, therefore, that glutamate transporter in canine red cells has the stoichiometry in which the transport of one glutamate is accompanied by two

Na^+ ions and by the countertransport of one K^+ ion and one anion (OH^- or HCO_3^-) as in salamander glial cells (Bouvier *et al.*, 1992). Although F^- and Br^- increased the L-glutamate uptake, it is unlikely that these halides, including Cl^- and I^-, were coupled to the transport, since both the external and internal replacements exhibited the same effect to a similar extent (Fig. 7). In fact, strong stimulation of glutamate-dependent current by these halides was not coupled to the transport process and these anions were transported by glutamate-gated anion channel intrinsic to glutamate transporters (Wadiche *et al.*, 1995). Thus, only HCO_3^- was the possible substrate to couple with glutamate transport activity in canine red cells.

Possible regulation of the transport by HCO_3^- would occur in a variety of tissues depending on their metabolic state, including CO_2 production and its conversion to HCO_3^-. In particular, in tissues and cells exposed to relatively high level of O_2 and CO_2, enhancement of L-glutamate uptake by HCO_3^- may be helpful to protect the contents from oxidative damage in response to O_2 consumption and CO_2 production. The increase of intracellular L-glutamate has been shown to stimulate glutathione synthesis in endothelial cells (Barbour *et al.*, 1988) and canine red cells (Maede *et al.*, 1983) by releasing the feedback inhibition of γ-glutamylcysteine synthetase by glutathione (Maede *et al.*, 1983). In normal (LK) canine red cells, L-glutamate is not accumulated as in HK cells because the intracellular Na^+ and K^+ reverse to collapse the inward Na^+ and outward K^+ gradients due to complete loss of Na,K-ATPase during reticulocyte maturation (Inaba and Maede, 1986). In this stage, the L-glutamate transport system will excrete excess L-glutamate and L-aspartate since transport in the reverse direction seems to occur (Fig. 5). Thus, the Na^+ and K^+-dependent L-glutamate transport system in canine red cells plays a role in regulation of these amino acids and glutathione contents at the maturational stage from reticulocyte to red cell. Moreover, in other tissues and cells, the dependence of L-glutamate transport on Na^+, K^+, and HCO_3^- may be important because such ionic environments are closely related to energy metabolism

and respiration.

The canine red cell L-glutamate transport system also showed substrate specificity (Fig. 8) that was similar to those of several distinct glutamate transporters identified cloning strategies (Pines *et al.*, 1992; Storck *et al.*, 1992; Kanai and Hediger, 1992). The red cell transport system, however, showed a rather low sensitivity to dihydrokainate and DL-α-aminoadipate, which potently inhibited a glial transporter GLT-1 (Pines *et al.*, 1992) but not a neuronal one (Kanai and Hediger, 1992). The neuronal transporter, EAAC1, was originally cloned in rabbit intestine and was shown to be distributed to many tissues including brain, intestine, kidney, liver and heart (Kanai and Hediger, 1992). Although ubiquitous expression of EAAC1 would suppose that EAAC1-type transporter is elicited in canine red cells, it is inconsistent with that L-cysteine, which is a selective inhibitor of human EAAC1 (Zerangue and Kavanaugh, 1996) , lacked inhibitory effect on red cell glutamate uptake (Fig. 8). Based on these observations, it is most likely that a glial glutamate transporter GLAST (Chaudhry *et al.*, 1995; Lehre *et al.*, 1995) would be the glutamate transporter in canine red cells. However, there has been no report on the existence of this subtype of glutamate transporter in peripheral tissues other than the central nervous system. Genetic identification is required to precisely determine molecular nature of the canine red cell glutamate transporter.

Chapter 2

Identification of Glutamate Transporter in Canine Red Cells

Introduction

Glutamate transporter gene family consists of GLAST, GLT-1, EAAC1, EAAT4, and EAAT5 (Storck *et al.*, 1992; Pines *et al.*, 1992; Kanai and Hediger, 1992; Fairman *et al.*, 1995; Arriza *et al.*, 1997). The first four subtypes are principally localized to the central nervous system and the last one is rather restricted to the retina. In the brain, glutamate transporters are highly differentially distributed, that is, GLAST and GLT-1 are specific to glial cells (Pines *et al.*, 1992; Chaudhry *et al.*, 1995; Lehre *et al.*, 1995), and EAAC1 and EAAT4 are found in neurons (Kanai and Hediger, 1992; Fairman *et al.*, 1995).

The findings in Chapter 1 have demonstrated that Na^+-dependent glutamate transporter in canine red cells has functional properties representing those of the transporters in the brain. Based on its pharmacological characteristics, it appeared most likely that canine red cell glutamate transporter was GLAST as discussed in the preceding Chapter. In this Chapter, isolation and identification of the cDNA were conducted to unambiguously define the molecular nature of the red cell glutamate transporter. First, canine brain and bone marrow cDNAs were subjected to PCR-based cloning of cDNA clones for GLAST, GLT-1, EAAC1, and EAAT4, assuming that the brain and erythroid cells share one of those transporter subtypes. Then, kinetic and pharmacological characterization of canine counterparts in *Xenopus* oocyte expression system and determination of tissue distribution of their transcripts were performed to elucidate the molecular feature of red cell transporter, followed by verification by immunological detection and identification of the transporter protein.

Materials and Methods

Dogs Some pure Shiba, Beagle and Japanese mongrel dogs were used. These dogs were clinically healthy and hematological parameters of their red cells were within reference ranges.

Isolation of RNA and DNA, reverse transcription, and PCR Methods for isolation of total RNA, poly(A)+ RNA, and genomic DNA, reverse transcription, PCR, and cloning of PCR products were as described in previously (Inaba *et al.*, 1996). RNAs were treated with DNase I. DNA sequencing was carried out using a Thermo Sequenase fluorescent labeled primer cycle sequencing kit with 7-deaza-dGTP (Amersham Pharmacia Biotech, Buckinghamshire, United Kingdom) on an automated DNA sequencer ALF express (Amersham Pharmacia Biotech, Uppsala, Sweden), or using a BigDye primer or terminator cycle sequencing kit (Perkin-Elmer Applied Biosystems, Foster City, CA, U.S.A.) on a 377A DNA sequencer.

PCR amplification of cDNA fragments of glutamate transporters To obtain partial cDNA sequences of canine transporter subtypes, cDNAs from the brain were amplified using degenerate primers designed according to the sequences of previously identified clones including rat GLAST (Storck *et al.*, 1992), rat GLT-1 (Pines *et al.*, 1992), rabbit EAAC1 (Kanai and Hediger, 1992), and human EAAT4 (Fairman *et al.*, 1995).

Poly(A)$^+$ RNA from canine forebrain cortex was reverse-transcribed using oligo(dT)$_{12\text{-}18}$ primers and SuperScript II reverse transcriptase (Life Technologies, Rockville, MD, U.S.A.) and amplified with PCR to detect cDNA fragments of GLAST, GLT-1, EAAC1, and EAAT4. Primer pairs used were as follows: GLAST, 5'-ACC AC(C/T) ATC ATT GCT GTG GTG-3' and 5'-GC(A/G) GTC CCA TCC ATG TTA ATG-3', corresponding to nt 388-408 and nt 1,208-1,188 of rat GLAST, respectively (Storck *et al.*, 1992); GLT-1, 5'- CTG GAT GCT AAG GCT AGT GGC CGC-3' and

5’-GC(A/G) GTC CCA TCC ATG TTA ATG-3’, corresponding to nt 322-345 and nt 1,202-1,183 of rat GLT-1, respectively (Pines *et al.*, 1992); EAAC1, 5’-GG(A/C/G/T) GAA ATC CTG ATG AGG ATG CTG-3’ and 5’-GC(A/G) GTC CCA TCC ATG TTA ATG-3’, corresponding to nt 165-188 and nt 1,111-1,092 of rabbit EAAC1, respectively (Kanai and Hediger, 1992); and EAAT4, 5’-GG(A/C/G/T) GAA ATC CTG ATG AGG ATG CTG-3’ and 5’-GGG GAA GGG GTT CCG GTG AGT GAC-3’, corresponding to nt 277-300 and nt 1,116-1,093 of human EAAT4, respectively (Fairman *et al.*, 1995). PCR-amplified fragments were cloned into pCR2.1 by the TA cloning method (Invitrogen, San Diego, CA, U.S.A.) and sequenced. The similarities of nucleotide sequences of each PCR product to rat GLAST, rat GLT-1, rabbit EAAC1 and human EAAT4 were 86.7, 86.6, 88.8, and 93.3%, respectively.

Rapid amplification of cDNA ends (RACE) reactions and constructions of the plasmid clones containing full open reading frames of glutamate transporter subtypes

Adapter-ligated cDNAs were prepared from poly(A)$^+$ RNA from the forebrain cortex of a dog, using a Marathon cDNA Amplification kit (CLONTECH, Palo Alto, CA, U.S.A.) according to the manufacturer's instructions. RACE reactions were performed using Advantage Klen Taq DNA polymerase (CLONTECH) with the adapter primers supplied by the manufacturer and gene-specific primers synthesized according to the sequences of the PCR-amplified cDNA fragments of canine brain glutamate transporters obtained as described above. The GLAST-specific primers for 5'- and 3'-RACE were EAT1p2 (5'-TGC CCC CCA ATT ACT CCC ATG TCT TCC-3', nt 938-912) and EAT1p1 (5'-ATT GTA CAA GTG ACA GCT GCA GAC GCC-3', nt 481-507), respectively. Nested primers were EAT1p4 (5'-TTT CCC TGC AAT CAG GAA GAG GAT GCC C-3', nt 900-873) for 5'-RACE and EAT1p3 (5'-AAA GTG CCC ATC CAG TCC AAT GAG ACG-3', nt 598-624) for 3'-RACE. PCR-amplified fragments were cloned into pCR2.1, and combined into pSPORT1 vector (Life Technologies, Inc., Rockville, MD, U.S.A.) to create 5'- and 3'-stretched canine brain

GLAST cDNA, pcGLAST. A bone marrow GLAST cDNA clone (pcGLASTbm) was also prepared in the same manner using poly(A)$^+$ RNA from bone marrow cells as the starting material. The GLAST cDNA fragments containing the coding region in full length were also obtained by PCR using a primer pair of EAT1p5 and EAT1p6 (see Table 1 and Fig. 9).

Likewise, 5'- and 3'-RACE reactions were performed to isolate and analyze cDNA clones of other canine brain transporter subtypes. Finally, cDNA clones containing full-length coding regions of canine GLT-1 (pcGLT-1), EAAC1 (pcEAAC1), and EAAT4 (pcEAAT4) were isolated. The sequences and positions of the primers utilized in cloning of these clones are shown in Table 1 and Fig. 9.

The complete nucleotide suqences of canine GLAST, GLT-1, EAAC1, and EAAT4 have been submitted to the GenBank™/EBI Data Bank with accession numbers AF067847 (canine GLAST cDNA), AF167076 (canine GLT-1 cDNA), AF107675 (canine EAAC1 cDNA), and AF107677 (canine EAAT4 cDNA).

Expression of canine glutamate transporter in Xenopus oocytes Oocytes (stage V-VI) were isolated from *Xenopus laevis* under ice-cold anesthesia and defolliculated by treatment with 0.2% collagenase (Type I-A, Sigma, St. Louis, MO, U.S.A.) in ND96 (96 mM NaCl, 2 mM KCl, 1 mM $MgCl_2$, 5 mM Hepes/Tris, pH7.5). The oocytes were microinjected with 10-25 ng (in 50 nl) of capped synthetic RNA of each glutamate transporter subtype. GLAST RNAs were transcribed from pcGLAST linearized with *Bgl* II immediately downstream of the termination codon using MEGAscript kit with T7 RNA polymerase and a cap analogue (Ambion, Austin, TX, U.S.A.). GLT-1 and EAAC1 RNAs were prepared from pcGLT-1 and pcEAAC1 linearized with *Bam*H I within vector sequences, respectively. For EAAT4 RNAs, *Hin*d III site within vector was used for linearization of pcEAAT4. The oocytes were incubated at 19°C in ND96 containing 1.8 mM $CaCl_2$, 100 units/ml penicillin and 100

μg/ml streptomycin for 36-72 hr.

RNA analysis by RT-PCR Total RNA (10 μg) from canine tissues were reverse transcribed using oligo(dT)$_{12-18}$ primers and Super Script II reverse transcriptase in a 25 μl-reaction. The resultant single-strand cDNA (0.5 μl) was amplified using *Taq* DNA polymerase at amplification conditions of denaturation at 94°C for 30 sec, annealing at 65°C for 30 sec and extension at 72°C for 1 min for 30 cycles or 40 cycles in a 25-μl reaction mixture. Primer pairs used for subtype specific PCR were as follows: EAT1p1 and EAT1p2 for GLAST, EAT2p1 and EAT2p2 for GLT-1, EAT3p1 and EAT3p2 for EAAC1, and EAT4p1 and EAT4p2 for EAAT4. Canine glyceraldehyde 3-phosphate dehydrogenase (GA3PDH) gene was also amplified as an internal control at the same conditions for 25 cycles using primers (5'-TGC TCC TTC TGC T GAT GCC CCCAT-3' and 5'-TCT GGG TGG CAG TGA TGG CAT GGA-3') prepared according to the sequence reported by Grone *et al* (1996). Ten-microlitter aliquots of PCR products were analyzed on 2% agarose gel. The remaining products were sequenced to confirm the specificity of the products.

Preparation of antibodies to canine GLAST Multiple antigen peptides were synthesized using Fmoc solid phase method for the amino acid sequence of carboxyl-terminal region of canine GLAST (NH_2-Asn-Ser-Val-Ile-Glu-Glu-Asn-Glu-Met-Lys-Lys-Pro-Tyr-Gln-Leu-COOH; residues 511-525, see Fig. 10) using a peptide synthesizer (Shimadzu, Kyoto, Japan) at Dr. Y. Takakuwa's laboratory (Tokyo Women's Medical University). New Zealand white rabbits were immunized with 100-

200 μg peptides with Freund's complete adjuvant followed by three successive immunization with Freund's incomplete adjuvant by 2 week intervals. Antisera were obtained 3 days after intravenous injection of the peptides. Anti-GLAST antibody was purified on an affinity chromatography media that were prepared by immobilizing synthetic peptides to N-hydroxysuccinimide-activated HiTrap column (Amersham Pharmacia Biotech) at the concentration of 1 mg/ml of packed gel. Antibodies bound to the column were eluted with 0.5 M NaCl, 0.1 M glycine/Tris, pH2.7 and neutralized immediately with Tris.

Analyses of membrane proteins Red cell ghosts were prepared as described (Inaba and Maede, 1986). Crude synaptic membranes from brain were prepared according to Kanner (1978). Membrane proteins were separated by 8% SDS-PAGE. The GLAST polypeptides were detected by immunoblotting using affinity-purified anti-GLAST antibodies and ECL chemiluminescence detection system (Amersham Pharmacia Biotech). In some experiments, membrane proteins were solubilized in 2% (w/v) CHAPS (Dojin Laboratories, Kumamoto, Japan) and kept on ice for 30 min to induce oligomerization of the GLAST proteins that lead to an efficient detection of the polypeptides with the antibodies. After addition of half volume of 3 x Laemmli's sample buffer, they were concentrated with ultrafiltration unit (Ultrafree MC, 30,000 nominal molecular weight limit, Millipore Corp., Bedford, MA, U.S.A.).

In vitro translation of canine GLAST pcGLAST was transcribed and translated

using TNT T7 coupled reticulocyte lysate system (Promega Corp., Madison, WI, U.S.A.) with or without canine pancreatic microsomes (Promega) in the presence of [^{35}S]methionine (EXPRE^{35}S^{35}S; 1,175 Ci/mmol, NEN Life Science Products, Boston, MA, U.S.A.). Translated products were analyzed by SDS-PAGE followed by exposure to Kodak BioMax MR films.

Deglycosylation studies Red cell membranes and crude synaptic membranes were deglycosylated using peptide:*N*-glycosidase F (PNGaseF; New England Biolabs, Beverly, MA, U.S.A.). Briefly, the membrane proteins (100-150 µg) were solubilized in 0.5% SDS, 1% β-mercaptoethanol at room temperature for 30 min. After addition of 1/10 volume of 10% Nonidet P-40 and 0.5 M Na phosphate, pH7.5, samples were incubated with 2,000 U of PNGase F at 37°C for 1 hr. Reactions were stopped by the addition of Laemmli's sample buffer and subjected to SDS-PAGE and immunoblotting.

Glutamate transport assay in red cells and Xenopus oocytes Uptake of L-glutamate in canine red cells was measured as previously described (Inaba and Maede, 1984).Oocytes injected with synthetic RNA were incubated at 19°C in ND96 medium containing L-[3,4-^{3}H]glutamate (49 Ci/mmol; NEN Life Science Products) and 1.8 mM $CaCl_2$ (100 µl/oocyte). After incubation, oocytes were washed three times with excessive amount of ice-chilled ND96 medium. Each oocyte was transferred into a 1.5 ml tube, lyzed in 200 µl of 1% SDS and radioactivity was determined using ReadyCap (Beckman, Fullerton, CA, U.S.A.). To estimate Na^+-independent transport, NaCl was

substituted by equimolar choline chloride. Under these conditions, the Na^+-dependent component, given by subtraction of the values in the absence of Na^+ from those in the presence of Na^+, increased linearly for the initial 5 min. Inhibitor sensitivity of the transporter was estimated by determining the transport activity for 5 μM L-glutamate in the presence of appropriate concentrations of various compounds, such as L- and D-glutamate, L- and D-aspartate, L-cysteine (Wako Pure Chemical, Osaka, Japan), *threo*-3-hydroxyaspartate (THA; Tocris Neuramine, Bristol, UK) and dihydrokainate (Sigma).

Table 1. Primers used to obtain canine Na^+/K^+-dependent glutamate transporter subtype cDNA clones.

Subtype	Primer	Sequence	Position
GLAST	EAT1p1	5'-ATTGTACAAGTGACAGCTGCAGACGCC-3'	481→507
	EAT1p2	5'-TGCCCCCCAATTACTCCCATGTCTTCC-3'	912←938
	EAT1p3	5'-AAAGTGCCCATCCAGTCCAATGAGACG-3'	598→624
	EAT1p4	5'-TTTCCCTGCAATCAGGAAGAGGATGCCC-3'	873←900
	EAT1p5	5'-CCCGAACACCCGGGCACAGTCGGCGAAG-3'	-120→-93
	EAT1p6	5'-TGTAAAACTAATTTCTTTTCTTTATTG-3'	3,632←3,658
GLT-1	EAT2p1	5'-GCCATGGTGTATTACATGTCCACAACCA-3'	331→358
	EAT2p2	5'-CCATCCTTGAACTCCAAGCCCTTCTTG-3'	663←689
	EAT2p3	5'-CTGGCCAGCTCCAAGCACGGGTGCGAG-3'	-74→-48
	EAT2p4	5'-AATCAAGAGGTGGTATTAAAAGAGGCACAG-3'	2,731←2,760
EAAC1	EAT3p1	5'-TGGGAAATATTCCGCAAGCTAGGCCTT-3'	826→852
	EAT3p2	5'-TTTCTTCTGCACAGCGGAAAGTGACAGG-3'	1,012←1,039
	EAT3p4	5'-TGGCTGAACTGGAAGAGATCATGAGAGC-3'	979←1,006
	EAT3p5	5'-CCCGCCATGGGCAAGCCGGCGAGGAAG-3'	-6→21
	EAT3p6	5'-GGGAAGGAGGAAGGGCAGAAGTATTTAT-3'	3,457←3,484
EAAT4	EAT4p1	5'-CACTCATTGTCTCCAGCCTGGTCACAG-3'	317→343
	EAT4p2	5'-TCTTGAACTGTTTGAAGCAGGCCTCCA-3'	572←598
	EAT4p3	5'-CCCTGGATAACAAGGCAACAGGGCG-3'	353→377
	EAT4p4	5'-GCAAAGGCCAGACTGACCCCAATG-3'	201←224
	EAT4p5	5'-TTGCAGTTGAGGCTCCCGATAGACG-3'	-25→1
	EAT4p6	5'-TTCCTGCTCCTTTATCTCAGTTTCCACCAAAC-3'	1,810←1,841

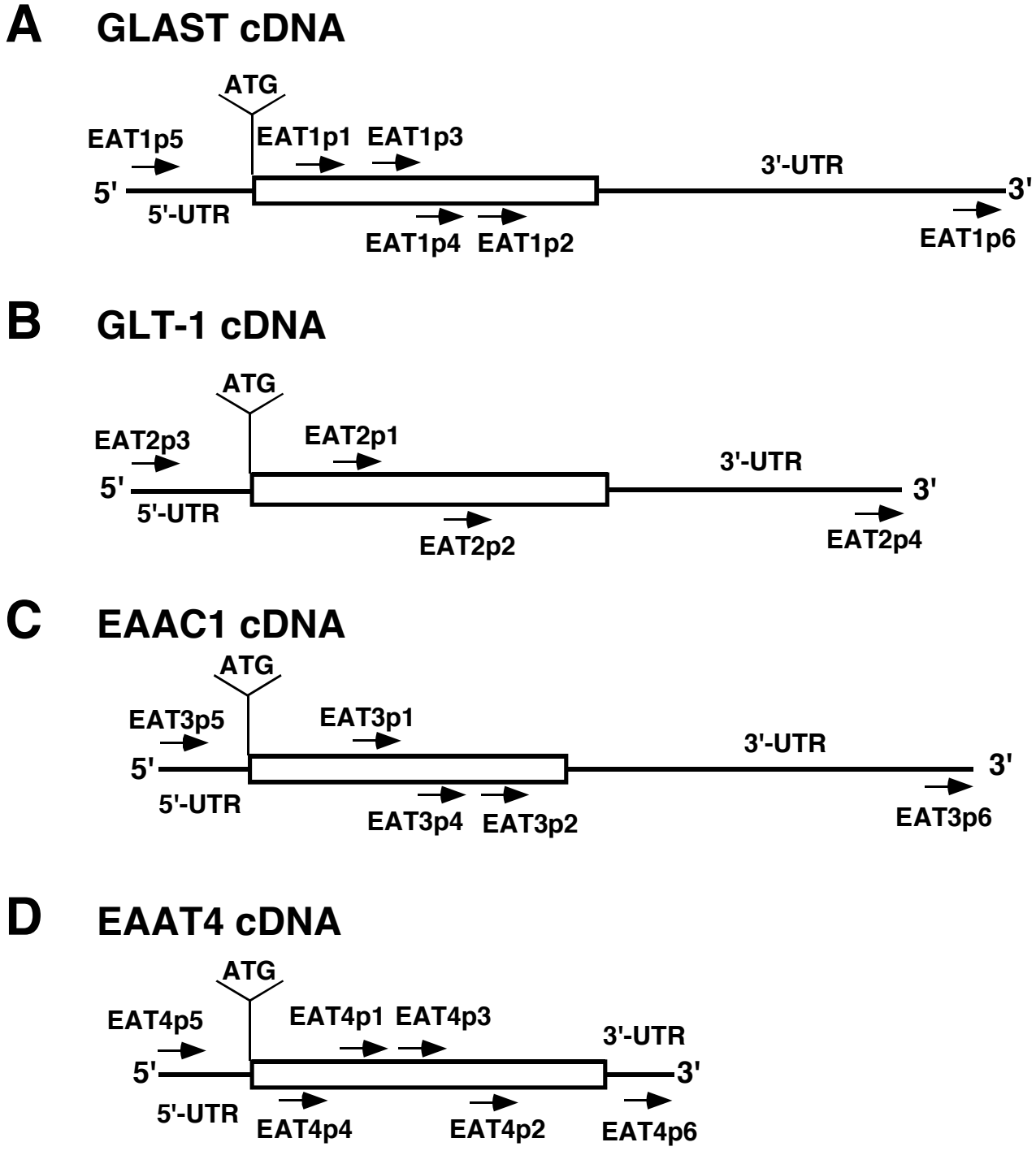

Figure 9. Positions of PCR primers for isolation of canine Na^+/K^+-dependent glutamate transporter subtype cDNA clones. Each Open box and solid lines represent coding resion, and 5'- and 3'-untranslated regions (UTR) of canine glutamate transporter subtype cDNA, respectively. The sense primers are shown as right-directed arrows and antisense primers are shown as left-directed arrows. Initiator ATG is indicated. Nucleotide position of each primer is listed in Table 1.

Results

Identification of canine red cell glutamate transporter

Isolation of cDNAs of canine brain glutamate transporter cDNA

PCR amplification of canine brain cDNA generated cDNA fragments corresponding to those of four different glutamate transporter subtypes, GLAST, GLT-1, EAAC1, and EAAT4. Nucleotide sequences of these cDNA fragments from dogs showed high similarities to those from other sources as described under "Materials and Methods." Based on the sequences obtained, primers specific to each glutamate transporter were prepared and 5'- and 3'-RACE reactions were carried out using canine brain cDNAs as templates. Thus, nucleotide sequences of cDNAs for canine GLAST, GLT-1, EAAC1, and EAAT4 were determined.

Figure 10 shows deduced amino acid sequences of four distinct glutamate transporters in dog brain with sequence similarities each other (48.1 - 65.7%). The deduced amino acid sequence of each subtype showed high similarity to those from other sources: canine GLAST, for example, had high similarity, over 96%, to human (Kawakami *et al.*, 1994), bovine (Inoue *et al.*, 1995), and rat (Storck *et al.*, 1992) homologues.

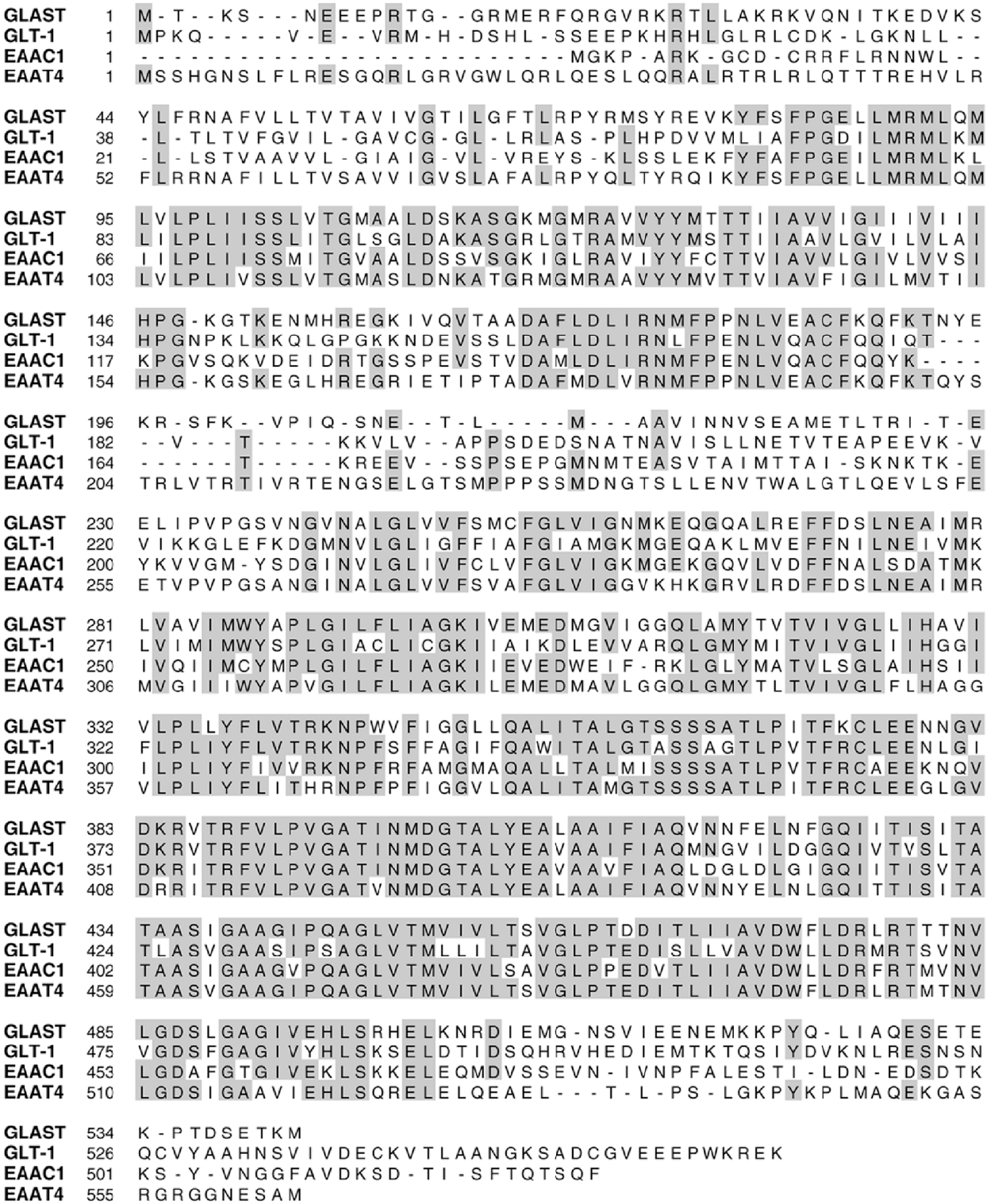

Figure 10. Alignment of deduced amino acid sequences of canine glutamate transporters. Amino acid sequences of canine GLAST, GLT-1, EAAC1, and EAAT4 deduced from nucleotide sequences of their cDNA clones all of which were isolated in this study were aligned. Conserved amino acid residues are shaded. Theoretical molecular masses of these transporters are 59,757 Da, 61,831 Da, 56,837 Da, and 61,435 Da for GLAST, GLT-1, EAAC1, and EAAT4, respectively. The complete nucleotide sequences of canine GLAST, GLT-1, EAAC1, and EAAT4 have been submitted to the GenBank™/EBI Data Bank with accession numbers AF067847 (canine GLAST), AF167076 (canine GLT-1), AF167075 (canine EAAC1), and AF167077 (canine EAAT4).

Characterization of glutamate transport by canine GLAST

Oocytes injected with synthetic RNAs of canine GLAST, GLT-1, and EAAC1 showed high-affinity Na^+-dependent glutamate uptake that was completely abolished when the extracellular Na^+ was replaced by choline. The Na^+-dependent uptake was dominated by a saturable component obeying Michaelis-Menten kinetics (Fig. 11). The *K*m values for L-glutamate obtained from Lineweaver-Burk plot were 36.3 μM, 55.6 μM, and 22.7 μM for GLAST, GLT-1, and EAAC1, respectively (Fig. 11). These values were slightly higher than that estimated for the uptake in canine red cells at 37°C (7-14 μM, (Inaba and Maede, 1984; Sato *et al.*, 1994), whereas lower affinity was reported for glutamate transporters expressed in oocytes (70-80 μM) (Storck *et al.*, 1992; Tanaka, 1993; Kawakami *et al.*, 1994; Inoue *et al.*, 1995). Since glutamate uptake by EAAT4 was not elicited even when the amount of synthetic RNA was increased to 50 ng/oocyte, EAAT4 was not analyzed further in the present study.

Several structural analogues of L-glutamate were tested for their inhibitory effects on glutamate transport to compare the pharmacological properties of glutamate transporter(s) in the brain and red cells (Table 2). Potent inhibition of the glutamate uptake was observed for GLAST, GLT-1, and EAAC1 in response to *threo*-3-hydroxyaspartate, L-glutamate, L- and D-aspartate but not by D-glutamate. These were the properties common to all the brain glutamate transporters (Kanai, 1997) and were also observed in canine red cells as described in Chapter 1. Dihydrokainate and L-cysteine inhibited the uptake of glutamate in oocytes injected with GLT-1 RNA and EAAC1 RNA, respectively, being compatible with previous findings that dihydrokainate and L-cysteine are selective inhibitors for human GLT-1 (Arriza *et al.*, 1994) and human EAAC1 (Zerangue and Kavanaugh, 1996), respectively. Whereas these agents poorly inhibited the glutamate transport by canine GLAST in oocytes and that in red cells. In addition, cysteinesulfinate, which reduced glutamate transport in

oocytes injected with GLAST also, inhibited the uptake of glutamate into red cells. Glutamate transport in canine red cells thus exhibited responses to the structural analogues, which were most consistent with those of the GLAST expressed in the oocytes (Table 2).

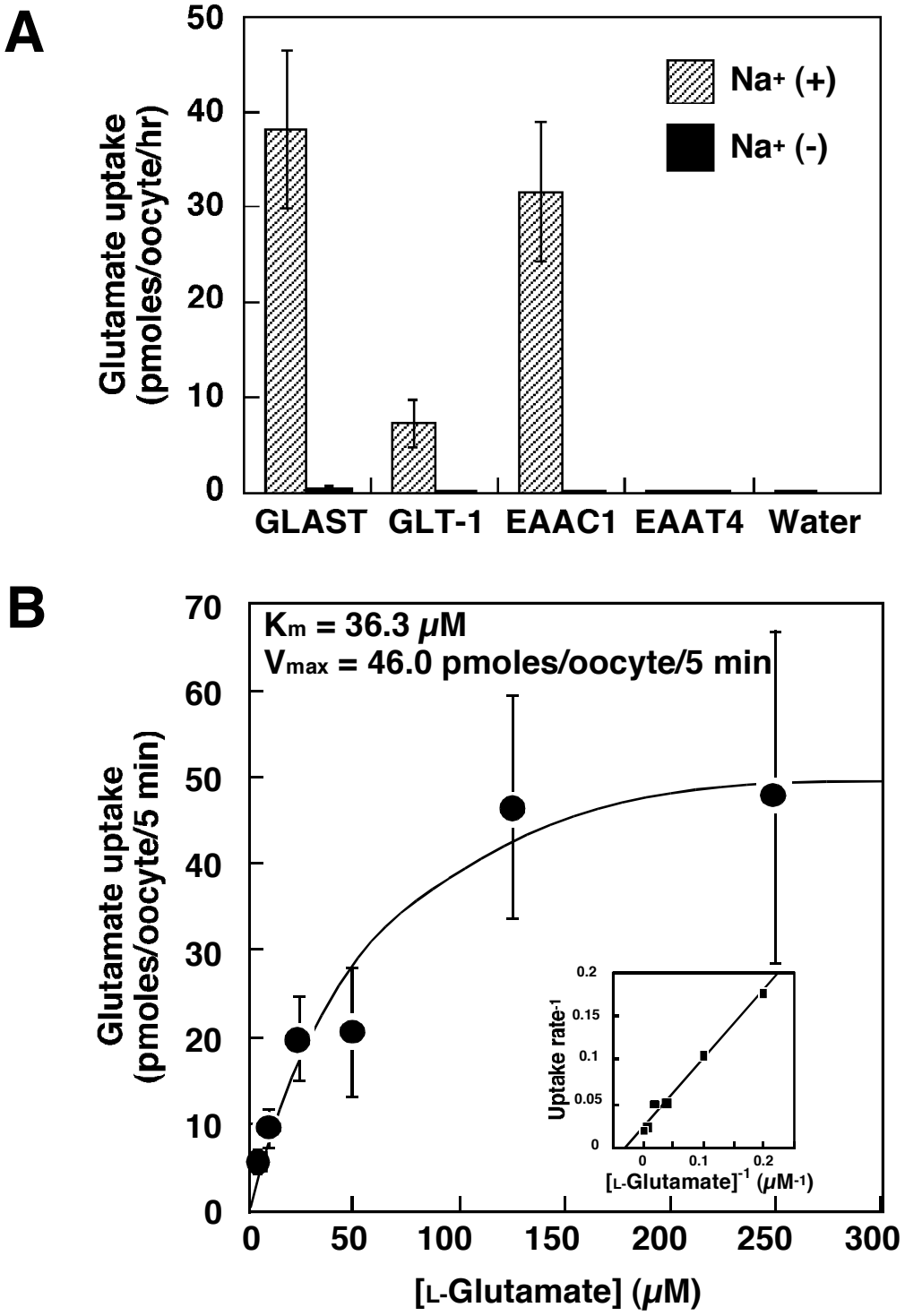

Figure 11. Kinetical analysis of L-glutamate transport in *Xenopus* oocytes expressing canine glutamate transporters. *Xenopus* oocytes were injected with 25 ng of synthetic capped RNA of GLAST (A and B), 10 ng of RNA of GLT-1 (A nd C), EAAC1 (A and D). After incubation for 48-60 hours, glutamate uptake was measured in ND96 medium containing L-[^{3}H]glutamate (5 μCi/ml) and various concentrations of L-glutamate at 19°C for 60 min (A), 5 min for GLAST (B) or 10 min for GLT-1 (C) and EAAC1 (D). Na^+-dependent uptake was calculated by subtracting the mean values in the absence of Na^+ from values obtained in the presence of Na^+. Data represent means ± S.D. (n = 6-8). Lineweaver-Burk plot of glutamate uptake by each isoform is shown in each inset.

C

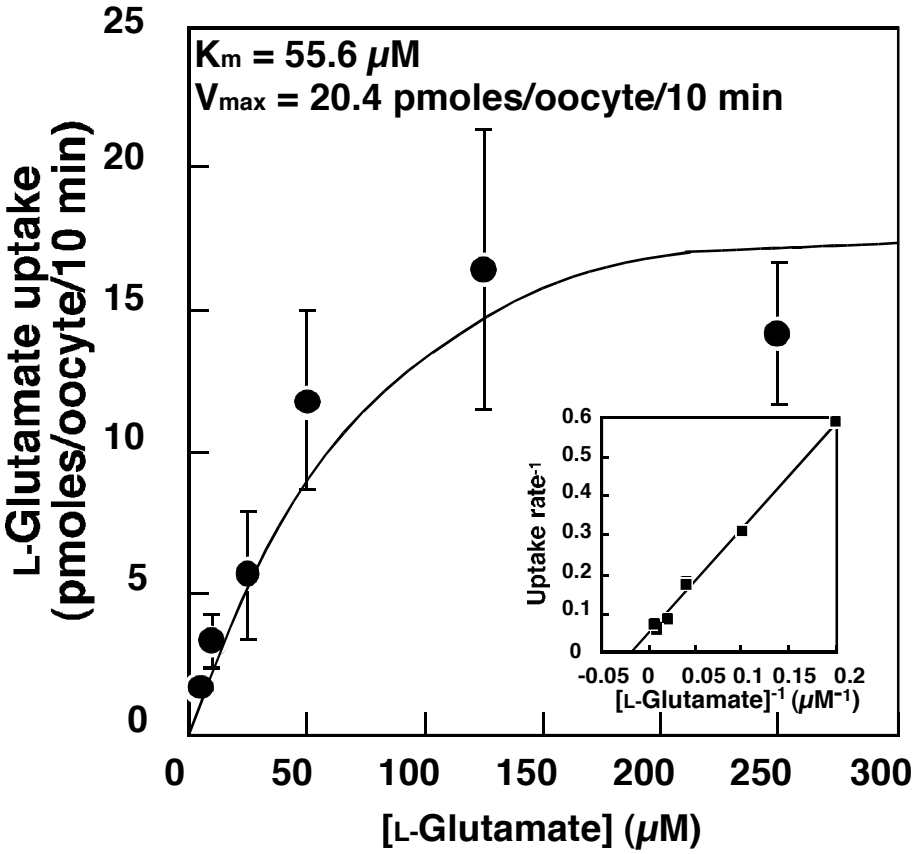
Km = 55.6 μM
Vmax = 20.4 pmoles/oocyte/10 min
L-Glutamate uptake (pmoles/oocyte/10 min)
[L-Glutamate] (μM)
Uptake rate-1
[L-Glutamate]-1 (μM-1)

D

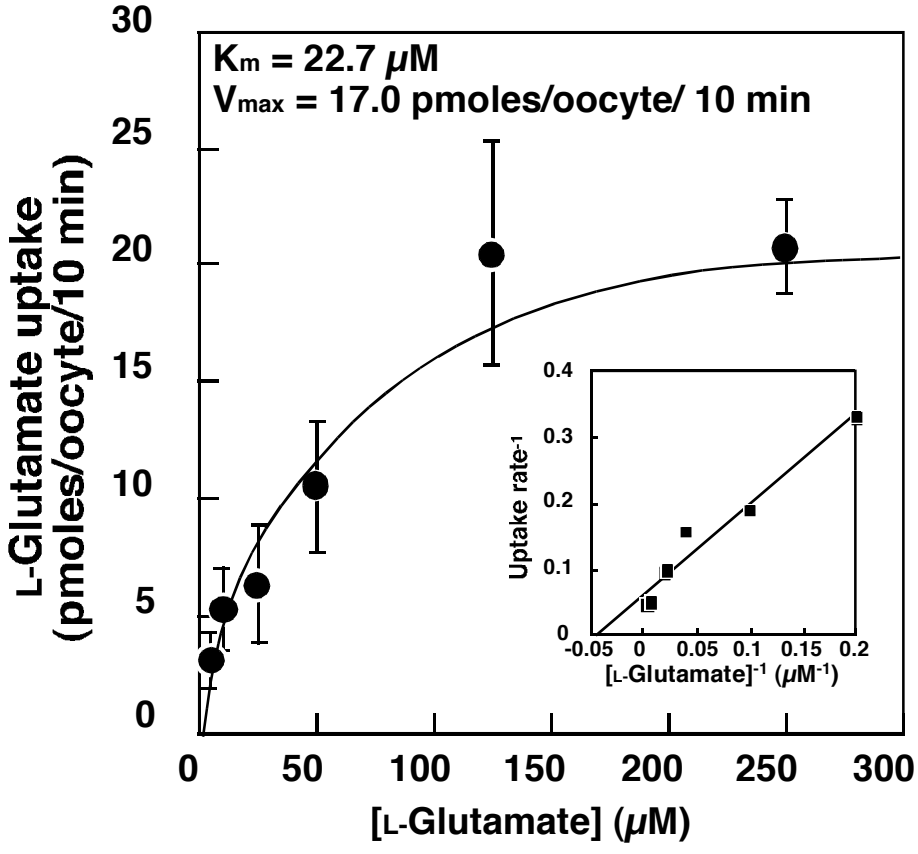
Km = 22.7 μM
Vmax = 17.0 pmoles/oocyte/ 10 min
L-Glutamate uptake (pmoles/oocyte/10 min)
[L-Glutamate] (μM)
Uptake rate-1
[L-Glutamate]-1 (μM-1)

Table 2. Cross-inhibition of canine glutamate transporters expressed in oocytes by structural analogues

	Activity (% of control)			
Inhibitors	GLAST	GLT-1	EAAC1	Red cells*
None (control)	100.0 ± 21.8	100.0 ± 10.2	100.0 ± 26.5	100.0 ± 5.0
L-Glutamate	46.3 ± 24.0	59.9 ± 38.3	65.6 ± 23.4	22.3 ± 0.3
D-Glutamate	87.8 ± 21.3	87.6 ± 25.6	87.1 ± 44.1	76.7 ± 11.8
L-Aspartate	43.9 ± 16.9	60.2 ± 1.7	48.2 ± 15.8	20.3 ± 0.9
D-Aspartate	61.5 ± 27.9	63.4 ± 4.3	51.7 ± 9.3	53.2 ± 2.2
threo-3-Hydroxyaspartate	15.7 ± 5.6	20.3 ± 4.8	40.9 ± 19.2	16.6 ± 0.4
Dihydrokainate (0.5 mM)	73.1 ± 21.2	19.7 ± 6.3	117.1 ± 31.9	56.4 ± 11.7 (1 mM)
L-Cysteine (0.5 mM)	73.3 ± 10.7	65.6 ± 12.4	42.9 ± 13.5	88.4 ± 1.0
L-Cysteinesulfinate	43.5 ± 6.0	N.D.**	N.D.**	20.6 ± 1.0

The uptake of 5 μM L-[^{3}H]glutamate was measured in oocytes expressing canine glutamate transporters (GLAST, GLT-1 or EAAC1) at 19°C for 5 min (GLAST) or 10 min (GLT-1 and EAAC1) in ND96 containing 25 μM of each analogue unless otherwise stated. Each value represents mean ± S.D. from 4-8 oocytes. *Reference data on dog red cells at 37°C (see Chapter 1). **N.D., not determined.

Analysis of mRNA expression by RT-PCR

RT-PCR analysis indicated amplification of cDNAs for GLAST, GLT-1, EAAC1, and EAAT4 with strong signals in the brain, i.e. the cerebral cortex, hippocampus, and cerebellum (Fig. 12). Amplification of GLAST cDNA was also observed in other tissues and cells except that a very faint band and no bands were obtained in reticulocytes and liver, respectively. It should be emphasized that signals for GLAST cDNA were detected clearly in reticulocytes and liver when the PCR cycles were increased (Fig. 12, right panels). Signals for GLAST cDNA fragments were also detected in all other tissues examined, including colon, spleen, pancreas, thyroid gland, adrenal gland, and testis, with intensities similar to those of reticulocytes and liver (data not shown). Under the PCR conditions employed, no noticeable amplification of the transporter cDNA other than that of GLAST cDNA was observed in bone marrow cells and reticulocytes, although EAAC1 showed a very faint band of PCR products in bone marrow after extended PCR cycles. These results demonstrated a ubiquitous expression of GLAST transcripts in a variety of cells and tissues in dogs and indicated that canine erythroid cells contained the GLAST mRNA but not the transcripts of other glutamate transporter genes. The cDNA clones from the brain (pcGLAST) and bone marrow cells (pcGLASTbm) isolated by 5'- and 3'-RACE reactions were both about 3.8 kb in length with a 1,629-bp open reading frame encoding a protein of 542 amino acid residues. The size of the GLAST mRNA was confirmed by Northern blotting although the signal intensity was very weak for bone marrow mRNA even when more than 10 μg of poly(A)$^+$ RNA was applied (data not shown).

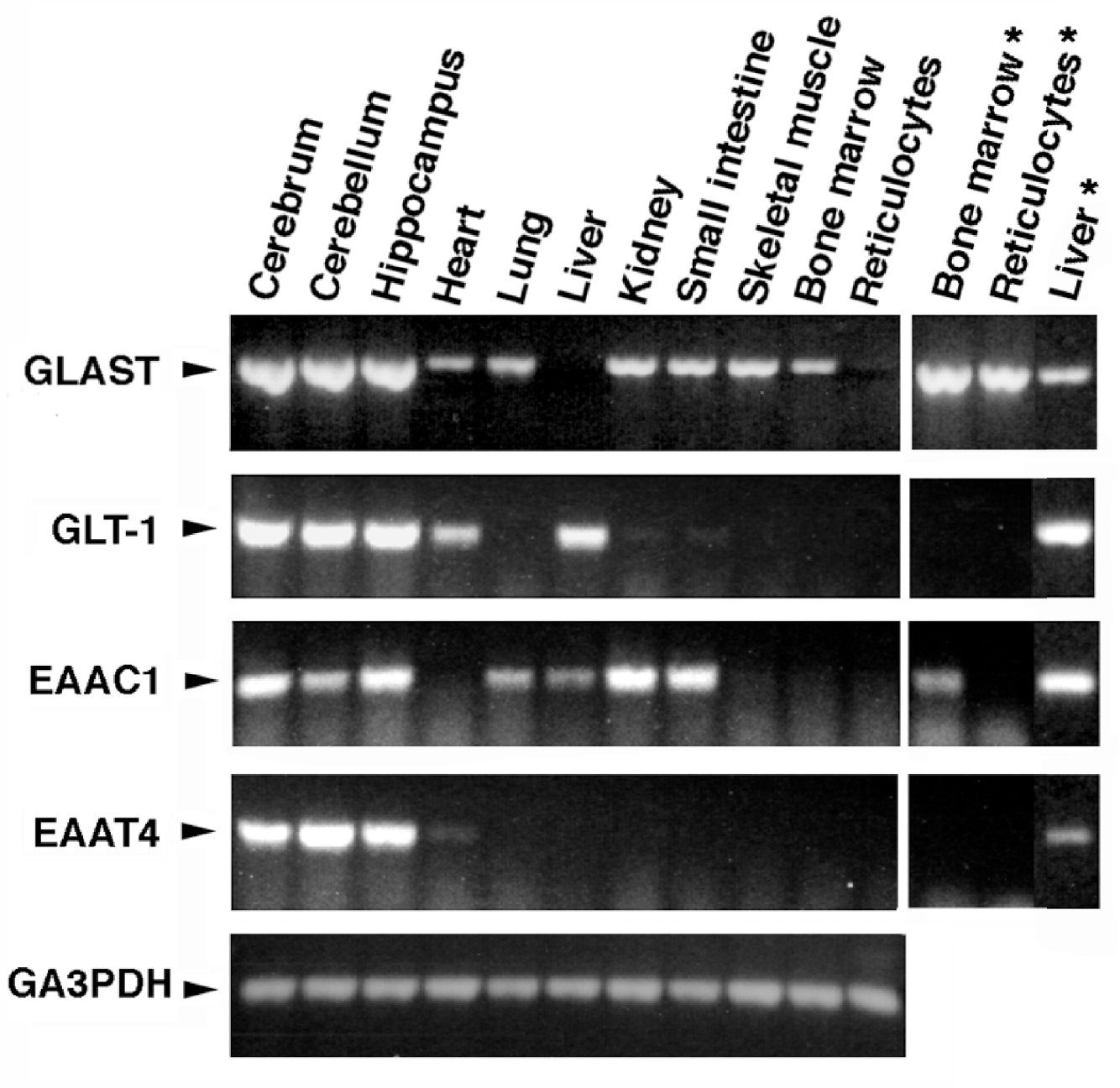

Figure 12. RT-PCR analysis for mRNAs of glutamate transporters in various canine tissues. mRNA of glutamate transporters was evaluated by RT-PCR using first-strand cDNA reverse-transcribed from total RNAs of various canine tissues. PCR amplification was carried out for 30 cycles. The results after 40 cycles (asterisk) are shown in the right panel. Canine glyceraldehyde-3-phosphate dehydrogenase (GA3PDH) cDNA was also amplified as the internal control for 25 cycles.

Identification of the GLAST protein in canine red cells

The findings described above suggested that the glutamate transporter in canine red cells was one of the subtypes, GLAST. To verify the presence of GLAST in red cells, antibodies specific to the GLAST protein were prepared and utilized in immunological identification of the polypeptide.

Affinity-purified antibodies to the synthetic peptide of GLAST reacted with 60-kDa proteins in membranes from the cerebral cortex, while the antibodies immunospecifically recognized polypeptides with an Mr of 66 kDa in red cell membranes, as documented in Fig. 13A (*Membranes*). When the brain membranes were solubilized with CHAPS, the distinct higher molecular mass signals at 120 kDa appeared on the immunoblot (Fig. 13A, *CHAPS extracts*) as reported for rat GLAST (Haugeto *et al.*, 1996). Likewise, 130-kDa bands appeared instead of the 66-kDa polypeptides in red cell membranes solubilized with CHAPS. The 130-kDa and 120-kDa bands were dimers presumably induced by oxidation of the thiol groups not reducible by sulfhydryl reducing agents as reported by previous investigators for rat GLAST (Haugeto *et al.*, 1996) and human GLT-1 (Trotti *et al.*, 1999). Additional bands at 96-100, 72, and 45 kDa were visualized in red cell membranes when a large amount of protein was loaded onto the gels. These bands were probably derived from nonspecific reactions of the antibodies with band 3, protein 4.2, and actin, respectively, because corresponding bands were also observed in human red cells that lacked Na^+-dependent glutamate transport activity (Fig. 13A).

It was interesting that the GLAST proteins synthesized in a reticulocyte lysate system had an Mr of only 50 kDa in our SDS-PAGE system (Fig. 13B), much less than those of the polypeptides immunospecifically recognized with antibodies and showed a mobility shift up to approximately 55 kDa when the translation reaction contained pancreatic microsomes (Fig. 13B), suggesting that *N*-glycosylation led to heterogeneity

in the Mr of GLAST proteins on SDS-gels. Actually, the Mr of the vast majority of the GLAST protein in cerebrum and cerebellum was reduced to about 50 kDa, consistent with that of the in vitro translation product, after removal of *N*-glycan with PNGase F (Fig. 13C). Based on the sequence similarity between canine and human GLAST as described above, recent models for membrane topology of human GLAST (Wahle and Stoffel, 1996; Seal and Amara, 1998) with 10 or 11 membrane spanning regions and cytoplasmic localization of N- and C-termini can be adopted to the canine homologue. This prediction supposes two potential *N*-glycosylation sites, at Asn206 and Asn216 with *N*-glycosylation consensus sequences (Asn-X, where X represents any residue except Pro-Ser/Thr) within the putative second extracellular loop. The inconsistency between the Mr of deglycosylated GLAST on SDS-gels (45 kDa or 54-57 kDa) and its theoretical molecular mass (60 kDa) has also been reported in the previous studies (Wahle and Stoffel, 1996; Schlag *et al.*, 1998). At present, I have no explanation for this phenomenon. Dimer bands in red cell membranes as well as those in brain membranes showed a reduction in their Mr to about 110 kDa after the treatment with PNGase F (Fig. 13C). These results showed that canine red cells had the 66-kDa GLAST protein (and its dimer) with *N*-glycan structures somewhat different from those in the brain. These findings evidently demonstrated that the glutamate transporter in canine red cells was GLAST.

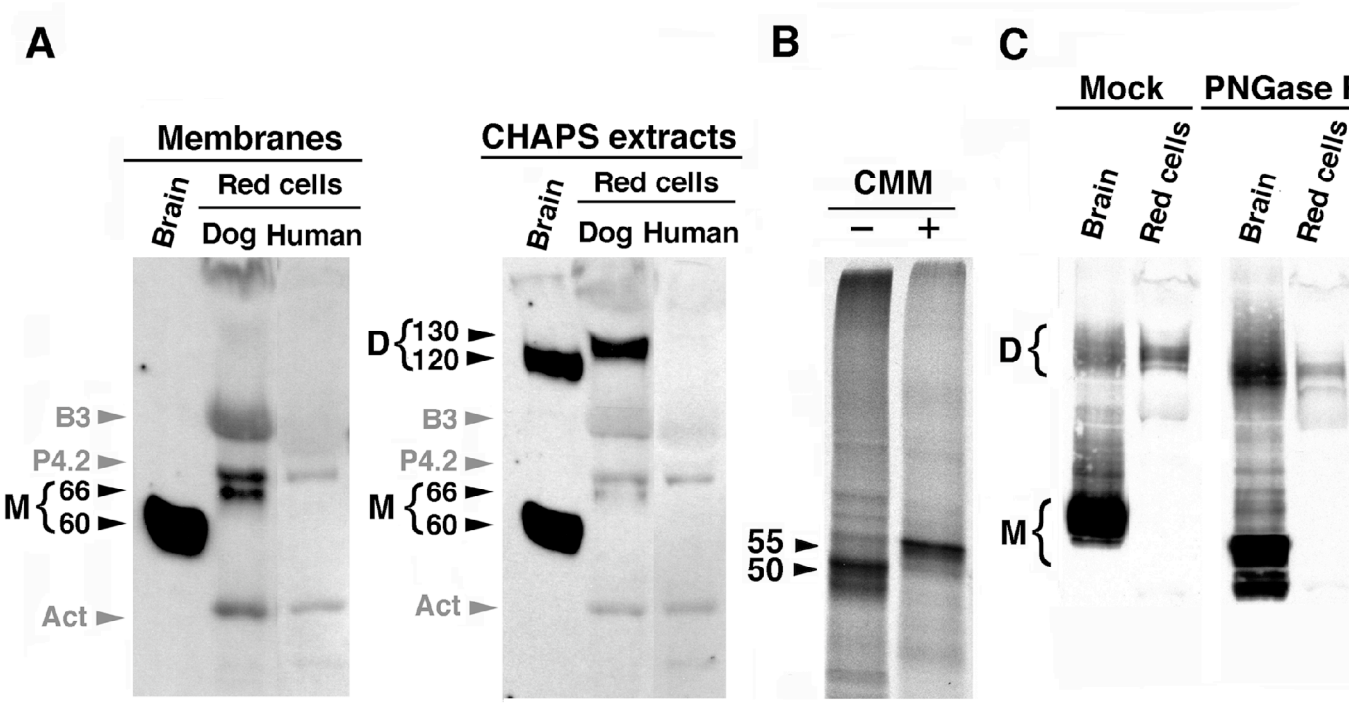

Figure 13. Analysis of canine GLAST proteins. A, membrane proteins from canine brain (cerebrum 1 μg each) and red cells (100 μg), and human red cells (100 μg) were separated by SDS-PAGE on 8% gels and transferred onto PVDF membranes (*Membranes*). GLAST proteins were detected using affinity-purified anti-C-terminal peptide of canine GLAST. Membrane proteins solubilized woth 2% CHAPS (*CHAPS extracts*) were also processed for immunoblotting. Monomers (M, 60 or 66 kDa) and dimers (D, 120 or 130 kDa) of GLAST polypeptides are indicated. Monomers (62 kDa) and dimers (120 kDa) were also detected in membranes from cerebellum (data not shown). Nonspecific bands corresponding to band 3 (100 kDa), Protein 4.2 (72 kDa), and actin (45 kDa) are indicated with gray arrowheads. B, in vitro synthesis of canine GLAST protein. Canine GLAST cDNA was transcribed and translated in a TNT reticulocyte lysate system with [^{35}S]methionine in the presence (+) and absence (-) of canine pancreatic microsomal membranes (CMM). The products were separated by SDS-PAGE and detected by autoradiography. C, removal of *N*-glycan from the GLAST proteins in brain and red cells. The crude membranes from cerebrum (5 μg), cerebellum (5 μg), and red cell ghosts (75 μg) were solubilized in 0.5% SDS, 1% β-mercaptoethanol at room temperature for 30 min. After addition of 1/10 volume of 10% Nonidet P-40 and 0.5 M Na phosphate, pH7.5, they were incubated at 37°C for 1 hour in the presence (*PNGase F*) or absence (*Mock*) of peptide:*N*-glycosydase F, followed by SDS-PAGE and immunoblotting. Migrating position of monomers (*M*) and dimers (*D*) of GLAST polypeptides are indicated with arrow heads.

Discussion

GLAST is one of the most abundant glutamate transporters in the central nervous system (Storck *et al.*, 1992) and has been believed to be rather specific to glial cells (Chaudhry *et al.*, 1995; Lehre *et al.*, 1995). The present study unequivocally demonstrated the presence of GLAST in a variety of peripheral tissues and cells, including red cells, as well as in the central nervous system. The molecular features of canine GLAST in erythroid cells and the brain were basically identical, and similar to those observed for previously identified GLAST homologues in terms of the affinity to glutamate, electrophoretic mobility on SDS-gel, and characteristic dimeric association upon solubilization (Figs. 11 and 13). Moreover, electrogenic properties and substrate specificity of the transport by canine GLAST (Table 2, see also Fig. 8 in Chapter 1, and (Inaba and Maede, 1984) are also consistent with those of the counterparts in human and rat. To my knowledge, this is the first demonstration of the ubiquitous expression of this glutamate transporter subtype.

The observation that the GLAST transcripts in erythroid cells and the brain were identical in size and sequence suggests the use of the same promoter(s) in the brain and peripheral cells. Furthermore, the GLAST transcripts were found in all the tissues examined in the present study (Fig. 12). These are consistent with the previous finding that the promoter sequence of the 5'-flanking region of the murine GLAST gene has the characteristics of a housekeeping gene containing CCAAT box and GC-rich regions (Hagiwara *et al.*, 1996). However, transcriptional regulation of GLAST in erythroid cells of dogs would be somewhat different from those of other mammals including human whose red cells do not possess Na^+-dependent L-glutamate transport system (Young and Ellory, 1977). Although preliminary analysis of 5' upstream sequence of the canine GLAST gene revealed the presence of some motifs for transcription factors including CCAAT motif, GC-rich region, CACCC motif, CACC-binding protein motif, and GATA recognition site, exact mechanisms for

transcriptional regulation of canine GLAST remains to be determined.

Glutamate transporters contribute to the termination of excitatory transmission (Nicholls and Attwell, 1990) and the prevention of excitotoxic mechanisms of neuronal cell death (Szatkowski and Attwell, 1994). In addition to being transporters for glutamate, all of the glutamate transporter subtypes cloned to date involving GLAST also function as Cl^- channels (Wadiche *et al.*, 1995). The Cl^- influx is activated by glutamate, but is not thermodynamically coupled to the transport of substrates (Fairman *et al.*, 1995). Thus, as mediators of both transport and ion channel activities, glutamate transporters have the potential to modulate synaptic transmission through the simultaneous execution of multiple functions. In peripheral tissues, EAAC1 has been presumed to be a transporter in intestinal or renal epithelial cells, because its transcripts were found in those tissues (Kanai and Hediger, 1992). Although abundant distributions of EAAC1 RNAs in those tissues were exemplified in the current study (Fig. 12), signals for EAAC1 relative to those of GLAST appear to be much less in other peripheral tissues, indicating functional expression of GLAST in various tissues. Transport and absorption of acidic amino acids (Schneider *et al.*, 1980; Rajendran *et al.*, 1987) and in modulation of glutathione metabolism (Deneke *et al.*, 1987) are supposed to be elicited by GLAST in those tissues and cells. In canine red cells, function of GLAST would be a determinant of glutathione levels (Maede *et al.*, 1983; Inaba and Maede, 1984) and would provide resistance or susceptibility of red cells to different types of oxidative attacks (Maede *et al.*, 1989). The differential distribution of transporter isoforms (Fig. 12) with K_m values for glutamate which were very close each other (Fig. 11) also suggests that these transporters share their roles via some selective mechanisms including interactions with components of the plasma membrane or the cytoplasm in different organs.

GLAST, GLT-1, and EAAC1 exhibit redox-sensing properties (Trotti *et al.*, 1998). Glutamate uptake is regulated by the chemical redox state of reactive cysteine residues

in the transporter structure. Reversible interconversions of cysteines between the reduced and the oxidized state are accompanied by dynamic upward and downward changes of transport activity. These glutamate transporters appear to exist as homodimeric assemblies in which the subunits are noncovalently associated presumably through disulfide bonding, and spontaneous oxidation of the polypeptides causes the formation of covalent bonds (Haugeto *et al.*, 1996; Trotti *et al.*, 1999) which was also observed for canine GLAST as shown in Fig. 13. Therefore, disulfide bonds that affect the transport activity could form either between cysteine residues within individual monomers, between cysteines in different subunits, or between the subunits and novel proteins connected to them. Oxidative inhibition of glutamate transporters implies opposite functional consequences, as it would increase extracellular glutamate levels and continuous activation of the receptors, leading to neurodegenerative disorders. Interestingly, the present study showed that two of three cysteine residues in the GLAST protein, Cys186 and Cys375, are conserved among four different transporter subtypes (Fig. 10). Mutational analysis on these cysteine residues would provide some new insights into pathogenesis of neuronal disorders.

Chapter 3

Molecular Basis for Inherited Defects of GLAST in Canine Red Cells

Introduction

Dysfunction of glutamate transporters has been considered to be involved in the pathogenesis of neurodegenerative diseases such as amyotrophic lateral sclerosis (Lin *et al.*, 1998; Trotti *et al.*, 1998). Selective depletion of glutamate transporters in rats, particularly glial transporters GLAST and GLT-1, by chronic administration of antisense oligonucleotides (Rothstein *et al.*, 1996) or by gene disruption (Tanaka *et al.*, 1997; Watase *et al.*, 1998) led to the appearance of neurological symptoms. Moreover, recent studies have suggested a direct link between oxidation and neurodegeneration based on the vulnerability to biological oxidants and possible involvement of an SH-based redox regulatory mechanism of glutamate transporters including GLAST and GLT-1 (Trotti *et al.*, 1998). These findings and ubiquitous expression of GLAST demonstrated in the preceding Chapter suggest that dysfunction of GLAST would cause multiple disorders including neurodegeneration and oxidative injury in peripheral tissues in dogs.

Japanese Shiba and mongrel dogs have the HK red cell trait in an autosomal recessive manner (Maede *et al.*, 1983), whereas dogs usually possess LK red cells. HK red cells show accelerated Na^+/K^+-dependent glutamate/aspartate uptake due to an increased concentration gradient of Na^+ and K^+ across the plasma membrane, leading to marked accumulations of intracellular glutamate, aspartate, and glutamine (Maede *et al.*, 1983; Inaba and Maede, 1984). The increased concentration of glutamate further results in an elevated level of reduced glutathione and affects the redox state and protection against oxidative stress of the red cell (Maede *et al.*, 1989). Interestingly, these breeds also include dogs characterized by reduced (Fujise *et al.*, 1993) and nondetectable (K. Sato, M., Inaba, and Y. Maede, unpublished observation, Oct. 1991) red cell glutamate transport, generating variant HK cells without accumulation of glutathione. During a preliminary study in which dogs were screened for their HK/LK

phenotypes, red cell glutathione, and red cell glutamate transport, a family of dogs was found to contain individuals whose red cells with a decreased level of glutathione were deficient in Na^+-dependent glutamate transport (LGluT, low glutamate transport). Their red cells were readily accessible to oxidants such as acetylphenyl hydrazine and generated Heinz bodies much more than normal HK cells with normal glutamate transport (NGluT) activity did (K. Sato, M. Inaba, and K. Kagota, unpublished observation, Apr. 1999). Such a hereditary defect of the glutamate transporter in mammals has never been described.

The purpose of the study in this Chapter was to define the molecular cause that underlies the hereditary deficiency of red cell glutamate transport in those dogs. Based on the findings on molecular features of the red cell glutamate transporter (Chapter 2), the GLAST cDNAs from dogs with LGluT phenotype and expression of the GLAST protein in their red cells were analyzed.

Materials and Methods

Dogs Dogs used in this study were from a family of Japanese mongrel dogs which were mixed breed of Japanese Shiba. Some pure Shiba dogs and Beagle dogs were also used. These dogs were clinically healthy and hematological parameters of their red cells (Table 3) were within reference range except that HK red cells had mean corpuscular volume slightly larger than that of LK red cells as demonstrated before (Maede *et al.*, 1982).

Isolation of RNA and DNA, reverse transcription, and PCR Methods for isolation of total RNA, poly(A)+ RNA, and genomic DNA, reverse transcription, PCR, and cloning of PCR products were as described in previous Chapters. RNAs used in reverse transcriptase reactions were treated with DNase I.

Expression of canine glutamate transporter in Xenopus oocytes Expression of the GLAST clones and glutamate transport measurements were carried out as described in the "Materials and Methods" in Chapter 2. In some experiments, 10 μg/ml cycloheximide (Sigma) were included in culture medium up to 12 hrs.

Analyses of red cell membrane proteins Preparation of red cell ghosts, solubilization with CHAPS, SDS-PAGE, and immunoblotting were performed as described in "Materials and Methods" in Chapter 2.

Restriction enzyme assay Restriction enzyme assay was carried out to determine genotypes for G492S mutation. PCR fragments corresponding to nt 1,427-1,657 of canine GLAST cDNA were amplified using genomic DNA from dogs as the templates. The resulting PCR products were digested with *Ngo*M IV for 3 hrs at 37°C and separated on 4% agarose gel.

Quantitation of GLAST mRNA GLAST mRNA was quantitated by RT-PCR combined with 5'-nuclease assay or SYBR green detection using the GeneAmp 5700 sequence detection system (Perkin-Elmer Applied Biosystems, Foster City, CA,

U.S.A.). 5'-Nuclease assay of GLAST mRNA was carried out with PCR primers, 5'-AAT GTG TCG GAA GCC ATG GAG-3' (nt 646-666), and 5'-TTG ACC CCA TTC ACA GAC CCT-3' (nt 725-705) in the presence of TaqMan probe of 5'-ACA AGG ATC ACG GAG GAG TTG ATC CCA G-3' (nt 673-700) and was normalized with the amount of GAPDH mRNA.

Results

Pedigree analysis for NGluT and LGluT red cell phenotypes

Measurement of red cell glutamate transport in individuals of a family of Japanese mongrel dogs revealed the presence of a red cell phenotype with low glutamate transport (LGluT) as shown in Figs. 14 and 15. Dogs carrying red cells with the LK phenotype (dogs I-1, I-2, III-2, and III-3) and a dog with HK red cells (dog II-1) exhibited glutamate transport that was reduced to about 20-30% of that in the normal LK and HK cells, while red cells from other dogs in this family had transport activity within the reference ranges (normal glutamate transport, NGluT). Moreover, two purebred Shiba dogs had LGluT red cells in which glutamate transport was hardly detectable in routine uptake assays with 2-5 min of incubation (S-1 and S-2). Extended period of incubation showed that glutamate uptake into these cells linearly increased for 60 min with an initial uptake rate of approximately 10 pmol/ml cells/min which was 1/80-1/70 of that in NGluT/HK cells (Fig. 15). Pedigree analysis also shows that the LGluT phenotype was totally independent of HK/LK phenotypes (Fig. 14).

Hematological parameters of red cells from dogs in the family were within reference range except that HK red cells with NGluT phenotype had an increased mean corpuscular volume and a decreased mean corpuscular hemoglobin concentration (Table 3), indicating hydration of these cells, as demonstrated before (Maede *et al.*, 1982). Actually, NGluT/HK red cells (II-5 and III-4) showed an increased concentration of glutathione as high as 10 mmol/l cells. However, red cells with LGluT/HK phenotype (II-1 and S-2) showed reduced content of glutathione compared with NGluT/HK cells (Table 3). Particularly, red cells from an individual S-2 with markedly decreased glutamate transport activity had extremely reduced level of glutathione which was less than that in LK red cells (Table 3).

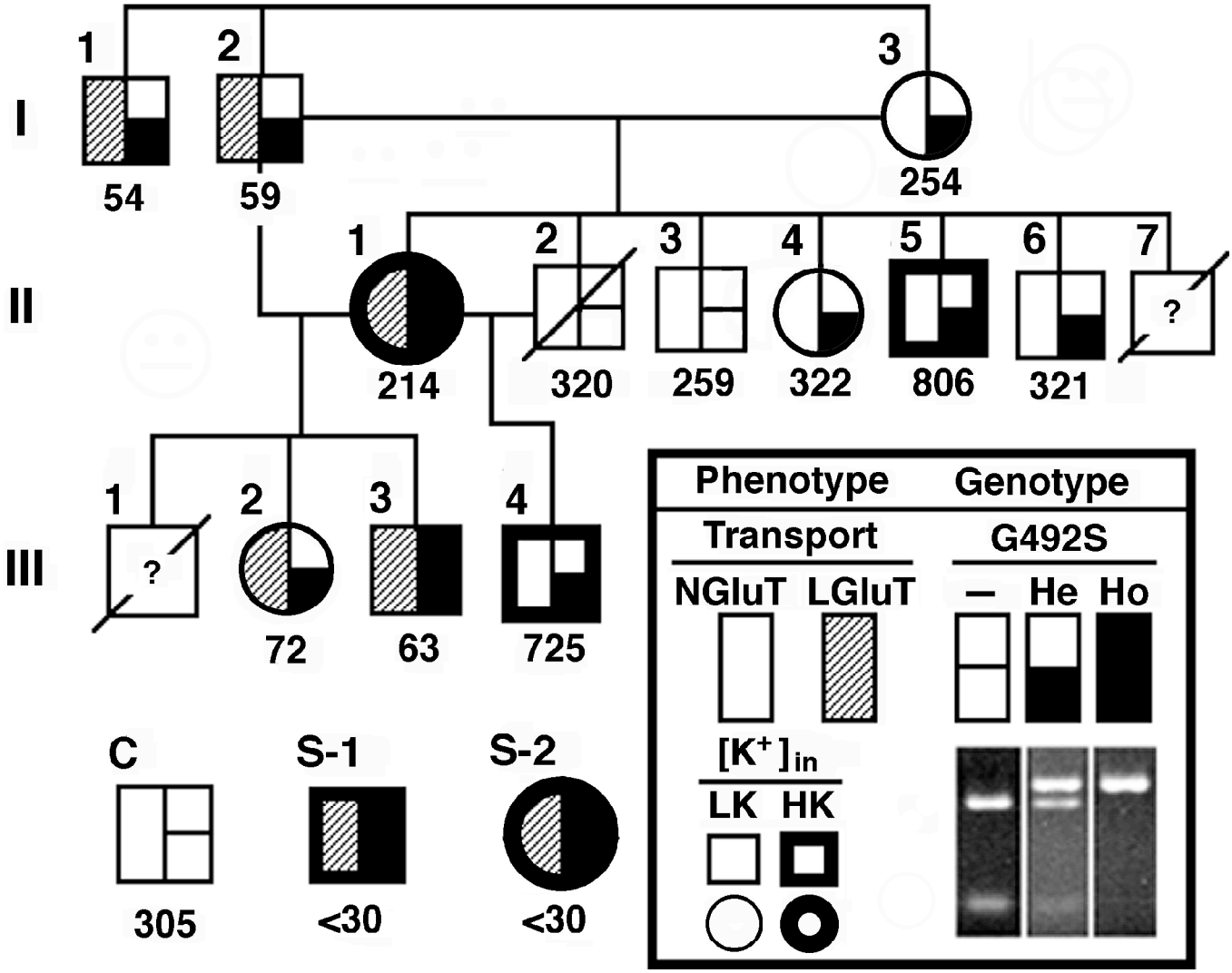

Figure 14. Pedigree of Japanese mongrel dogs including LGluT dogs. A family consisted of three generation (I-III) of Japanese mongrel dogs and some other dogs were studied. The value shown below each symbol represents Na^+-dependent glutamate transport activity in pmol/ml cells/min. Phenotypes for glutamate transport activity (NGluT and LGluT) are indicated in left side of each symbol. Individuals possessing HK phenotype red cells are indicated by thick line of the symbol. Genotypes for G492S mutation of GLAST was determined by PCR-RFLP (see text) and are indicated in right side half of the symbol. A typical profile of PCR-RFLP is shown in the insert.

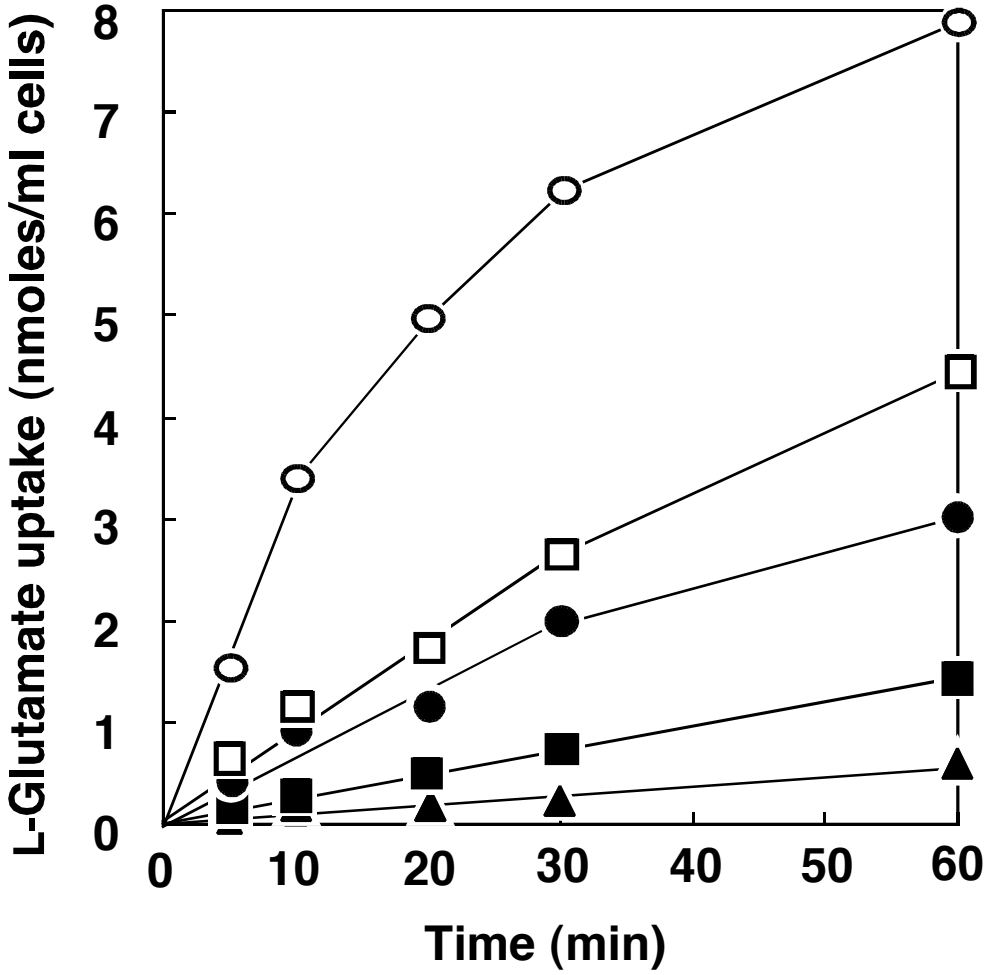

Figure 15 . Time course of L-glutamate uptake in canine red cells with various phenotypes . L-Glutamate uptake was measured in the medium containing 5 μM L-[^{3}H] glutamate (2 μCi/ml) at 37°C for the indicated periods. Na^+-dependent uptake was calculated by subtracting the mean values in the absence of Na^+ from values obtained in the presence of Na^+. Symbols indicate phenotypes LK/NGluT (□), LK/LGluT (■), HK/NGluT (○), HK/LGluT (●), and HK/LGluT (▲).

Table 3. Hematological parameters in various phenotype dog red cells

	HK/NGluT (n = 2)	HK/LGluT (n = 2)	LK/NGLuT (n = 4)	LK/LGluT (n = 4)
RBC (x $10^6/\mu$l)	6.46	6.88	7.78 ± 0.60	7.58 ± 0.89
Hb (g/dl)	14.0	14.5	17.0 ± 1.3	17.0 ± 1.7
Hct (%)	51.0	49.3	51.0 ± 3.8	52.0 ± 4.8
MCV (fl)	78.0	71.8	66.0 ± 1.7	69.0 ± 2.0
MCH (pg)	22.0	21.2	21.0 ± 0.5	22.0 ± 0.5
MCHC (g/dl)	28.0	29.5	33.0 ± 0.4	32.0 ± 0.5
GSH (mmol/l cells)	9.5	5.6 (II-1), 1.3 (S-2)	2.1 ± 0.4	1.9 ± 0.3

Data are expressed as mean values (± S.D.). Abbreviations used areas follows: HK, intracellular high K^+; LK, intracellular low K^+; NGluT, normal glutamate transport; LGluT, low glutamate transport; RBC, red blood cells; Hb, hemoglobin; Hct, hematocrit; MCV, mean corpuscular volume; MCH, mean corpuscular hemoglobin; MCHC, mean corpuscular hemoglobin concentration; and GSH, reduced glutathione.

When red cells were incubated with 30 mM acetylphenyl hydrazine, turbidity of hemolysate showed an increase with a concomitant increase of Heinz body count (Maede *et al.*, 1989). The increase of turbidity and Heinz body count in HK red cells with a high concentration of glutathione was far less than those observed in LK red cells, while LGluT red cells from HK dogs (II-1 and S-2) showed a remarkable increase in Heinz body formation (Fig. 16). Typically, turbidity of hemolysate from LGluT/HK red cells of S-2 was about 2.5-fold that of normal LK cells and 6-fold that of normal HK cells: most of all red cells from a dog S-2 contained more than 5 Heinz bodies after incubation with acetylphenyl hydrazine for 6 hrs. These results indicated that defective glutamate transport is responsible to the decreased level of reduced glutathione, ultimately facilitating oxidative damage in red cells.

The GLAST protein levels in canine red cells with inherited reduced glutamate transport

Immunoblotting using antibodies to the GLAST peptide demonstrated that CHAPS extracts of red cells with normal transport contained the GLAST dimers (130 kDa) at fairly detectable levels, whereas red cells from LGluT dogs gave only faintly visible bands for the GLAST dimers (Fig. 17). Densitometric scanning of the immunoblot indicated that the content of immunoreactive GLAST polypeptides detected as dimers in LGluT cells was much less than 10% of that in the NGluT red cells or was nearly totally missing. There was no significant difference between NGluT and LGluT red cells in terms of their major membrane protein profiles on SDS-gels stained with Coomassie Brilliant Blue. These findings indicated that impaired transport of glutamate in LGluT cells was in parallel with specific reduction of the GLAST protein content.

Genetic analysis of the GLAST cDNA from dogs with reduced red cell glutamate transport

Sequencing analysis of the GLAST cDNA clones isolated from bone marrow cells of some LGluT dogs showed a missense mutation of G to A at nucleotide 1,594 that generated substitution of Gly492 to Ser (G492S). This mutation was confirmed by restriction enzyme assay of the PCR products from genomic DNA. It was not likely that this mutation was a simple polymorphism, since none were identified in genomic DNAs from 50 control dogs other than Shiba and Japanese mongrel dogs. However, pedigree analysis indicated that this G492S substitution did not simply cosegregate with the red cell phenotype of reduced glutamate transport by itself, since while red cells from individuals II-1, III-2, S-1, and S-2, homozygous for this mutation, exhibited the LGluT phenotype, the heterozygous state resulted in either LGluT or NGluT red cells (Fig. 14). Therefore, we analyzed mRNA levels and characteristics of G492S GLAST to figure out significance of this mutation.

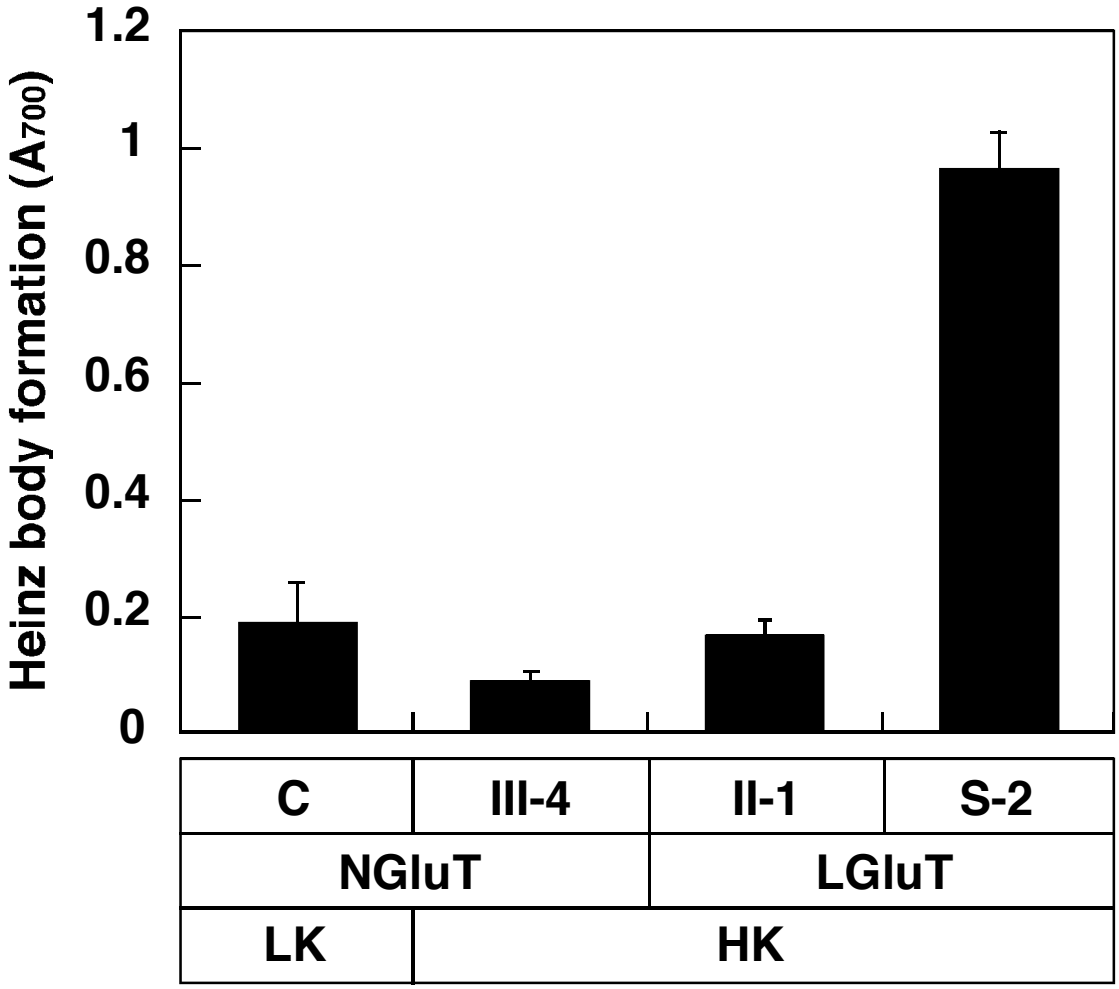

Figure 16 . Effects of acetylphenylhydrazine on the formation of the Heinz bodies in dog red cells. Red cells were incubated with 30 mM acetylphenylhydrazine at 37°C for 3 hrs. The turbidity of the red cell lysates was determined by measuring the difference in absorbance of the hemolysate at 700 nm before and after centrifugation at 12,000 x g for 3 min (See "Materials and Methods").

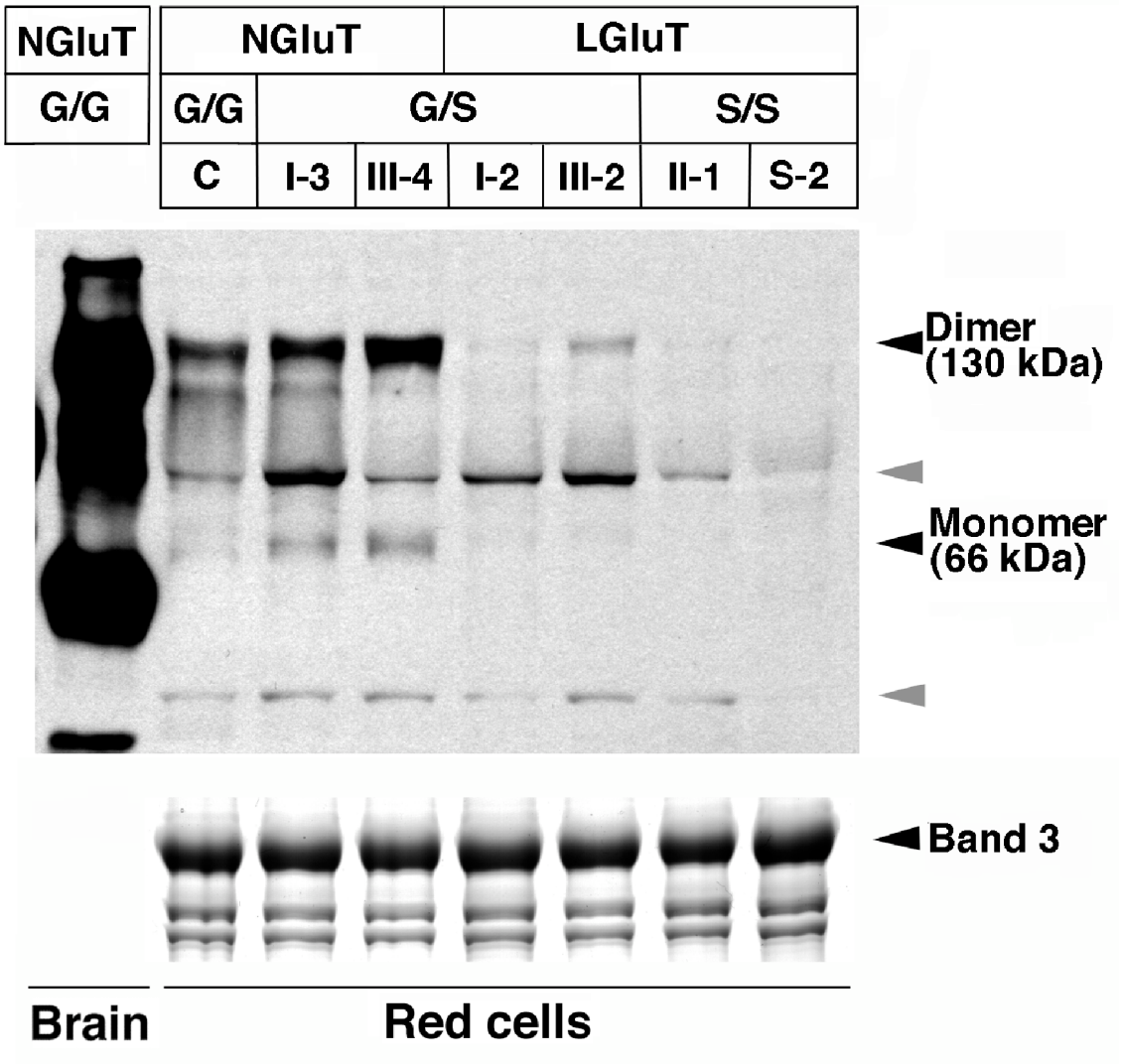

Figure 17. Immunoblot analysis of the GLAST protein in LGluT red cells. Red cell membranes (100 μg) from dogs shown in Fig. 14 were solubilized in 2% CHAPS and concentrated by ultrafiltration after addition of Laemmli's sample buffer. Proteins were separated on 8% SDS-gels and the GLAST proteins were detected using affinity-purified anti-GLAST antibodies. Black arrows indicate GLAST monomers and dimers, and shaded arrows indicate nonspecific bands. NGluT and LGluT traits, genotypes for G492S mutation, and individual identifications are indicated. G/G, G/S, and S/S represent free (wild type), heterozygous, and homozygous for G492S mutation. The lower panel shows band 3 (100 kDa) region of Coomassie brilliant blue-stained gel for comparison.

Quantitation of GLAST mRNA in bone marrow cells

To quantitate GLAST mRNA levels in bone marrow cells, we employed a 5'-nuclease assay using TaqMan probes because the relative abundance of GLAST transcripts was insufficient for estimation by Northern blotting as described in Chapter 2. As shown in Fig. 18A, copy numbers of the GLAST mRNA, determined by amplification of the nt 646-725 sequence, in LGluT dogs heterozygous for G492S mutation were remarkably decreased compared to those in NGluT dogs. A similar decrease in total GLAST mRNA was also observed in an LGluT dog homozygous for G492S (S-2), while relative abundance of the GLAST mRNA in individual II-1 (homozygous for G492S, LGluT phenotype) was apparently increased.

PCR amplification of another target sequence including the G492S locus (nt 1,427-1,657) gave a similar result (data not shown). Digestion of this sequence with *Ngo*M IV (or *Nae* I) showed that GLAST transcripts from the G492S allele were obviously abundant in the amplification products of LGluT dogs, while PCR products of NGluT dogs carrying the G492S mutation had digestion profiles indistinguishable from those of genomic DNA (Fig. 18B). This indicated that a selective decrease in accumulation of GLAST mRNA with a normal coding frame occurred in LGluT dogs heterozygous for G492S mutation, suggesting that some transcriptional defect of normal allele would contribute to generate decreased level of GLAST proteins in a subset of LGluT phenotype.

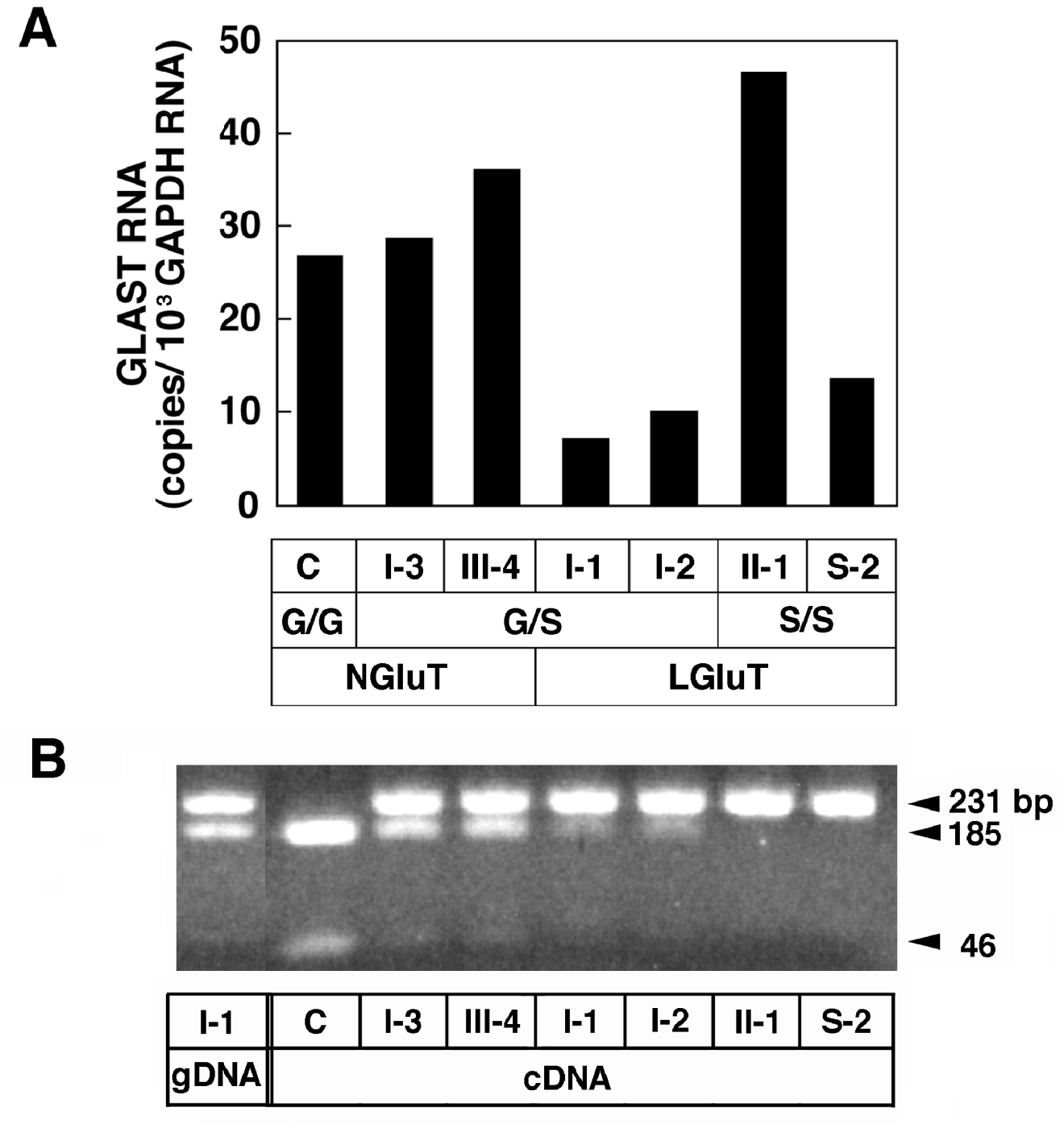

Figure 18. Quantitative analyses of GLAST mRNA by RT-PCR-based assay. A, GLAST mRNA in bone marrow cells of NGluT and LGluT dogs were quantitated by RT-PCR combined with a 5'-nuclease assay, and shown in copy numbers normalized for 1,000 copies of GAPDH mRNA. B, GLAST cDNA fragments containing G492S mutation locus were amplified from bone marrow cDNAs and were digested with *Ngo*M IV as in PCR-RFLP analysis for G492S genotyping (see legend for Fig.14). The digestion profile for the fragment amplified from genomic DNA of a dog heterozygous for G492S mutation is shown at left (*gDNA*). For abbreviations, see legend for Fig.17.

Functions and stability of G492S GLAST in Xenopus oocytes

Xenopus oocytes microinjected with synthetic RNA carrying G492S mutation showed glutamate uptake with kinetic constants similar to that of wild-type GLAST (Fig 19A). Co-injection of wild type and G492S RNA caused no significant alteration in transport activity. Furthermore, functional expression of G492S GLAST was observed in COS-7 cells (data not shown).

It was then examined whether the mutant protein was different from wild-type GLAST in terms of the stability or turnover rate. After incubation of oocytes for 12 hr in the presence or absence of cycloheximide, glutamate transport activity of the wild type was not affected by the addition of this translation inhibitor. However, glutamate uptake in the oocytes injected with G492S GLAST and incubated with cycloheximide was only about 60% of that in control oocytes incubated without cycloheximide, and was less than that observed before the addition of cycloheximide (Fig. 19B). It is not likely that the reduction in the activity of G492S GLAST was due to a decrease of the mutant RNA content within the oocytes since the transport activity of G492S GLAST was increased when oocytes were not exposed to cycloheximide, as observed for the wild type (Fig. 19B). These findings demonstrated that G492S GLAST was fully functional for Na^+-dependent glutamate transport but was unstable compared to the wild-type transporter.

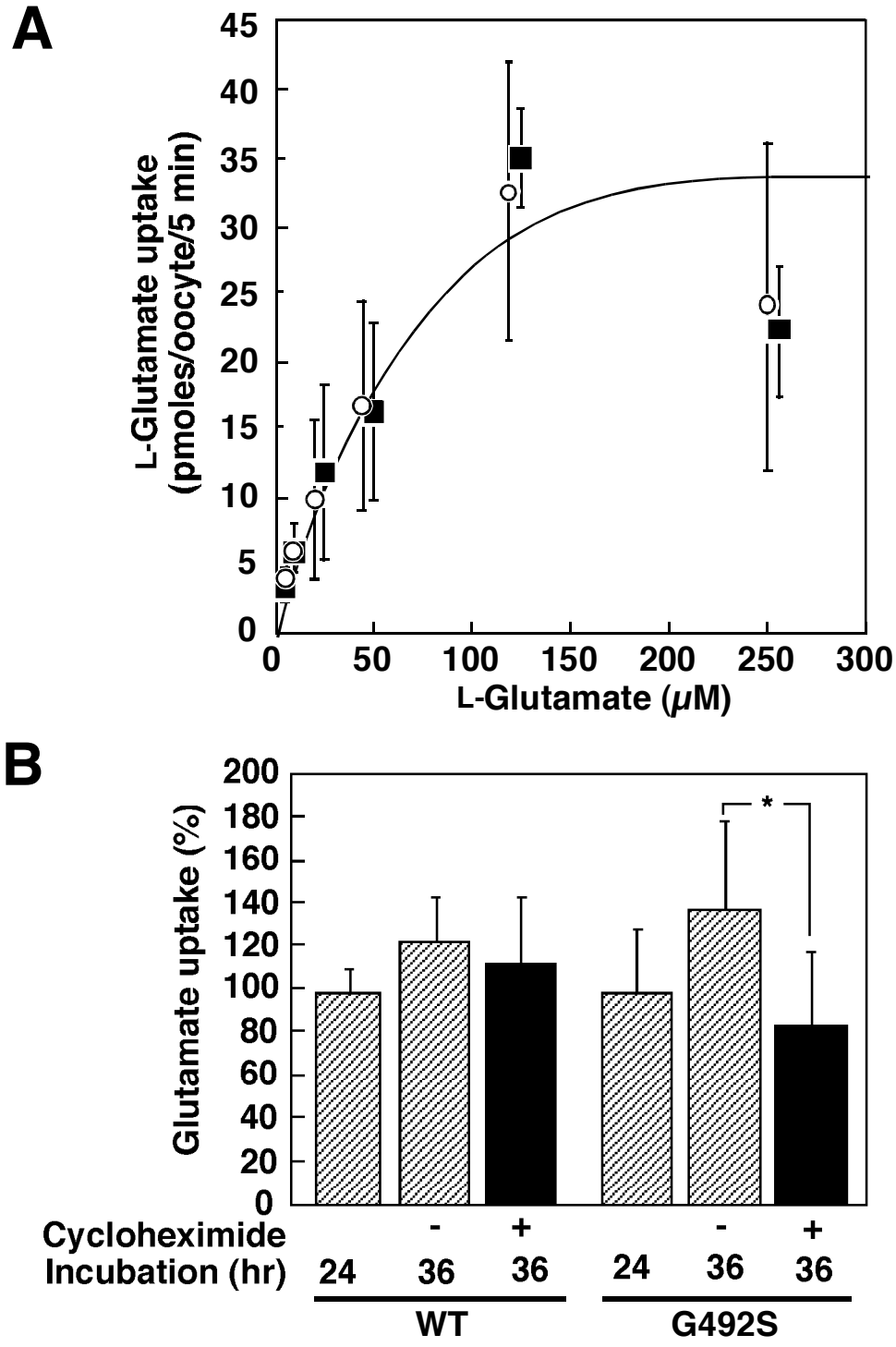

Figure 19. Characterization of G492S GLAST expressed in *Xenopus* oocytes. A, L-glutamate uptake into *Xenopus* oocytes injected with 25 ng of capped RNAs from wild-type (open circles) and G492S mutant (closed squares) GLAST. Uptake was measured as described in the legends for Fig. 11. No significant difference was observed in their kinetic constants (wild type vs G492S; K_m, 43.5 vs 38.6 μM; V_{max}, 32.6 vs 27.2 pmol/oocyte/5 min). B, the effect of cycloheximide on the activities of wild-type and G492S in oocytes. At 24 hr after injection of synthetic RNAs, glutamate uptake was measured, and the remaining oocytes were further incubated for 12 hrs in the presence or absence of 10 μg/ml cyclohexmide. Data are expressed as means ± S.D. (n = 8-16, $^*P < 0.05$) of the uptake value relative to the uptake at 24 hr after injection.

Discussion

Recent studies have shown that GLAST plays essential roles in the brain and retina for normal neurotransmission and protection of neuronal cells from the excitotoxicity of glutamate (Trotti *et al.*, 1998; Watase *et al.*, 1998; Harada *et al.*, 1998). The vulnerability to biological oxidants and possible involvement of an SH-based redox regulatory mechanism of glutamate transporters, including GLAST, have suggested a direct link between oxidation and neurodegeneration (Trotti *et al.*, 1998). Previous studies by Maede and hid colleagues (Maede *et al.*, 1983; Maede *et al.*, 1989) have suggested that glutamate transport in dog red cells regulates the synthesis and accumulation of reduced glutathione, affecting the susceptibility of the cells to oxidative stress. The present study demonstrated that LGluT red cells with the HK phenotype had glutathione content reduced to 15% (S-2) and 60% (II-1) (1.3-5.6 mmol/liter of cells, respectively) of that in HK cells with normal glutamate transport (Table 3). Typically, red cells from an LGluT/HK dog (S-2, Fig. 14) showed remarkably accelerated formation of Heinz bodies when incubated with acetylphenyl hydrazine, while NGluT/HK dogs had red cells resistant to this oxidative agent (Fig. 16). These findings and the identification of GLAST in canine red cells indicate that one of the physiological roles of GLAST in peripheral tissues is to modulate the antioxidative defense of the cells. In turn, they also suggest that neuroprotection by GLAST under physiological conditions may involve the glutathione metabolism.

The most interesting finding was that defective glutamate transport in LGluT dogs was associated with a decrease of the GLAST protein content in their red cell membranes (Fig. 18). This is convincing evidence for the previous observation that the difference in glutamate transport activity between HK cells and HK cells with a low glutathione concentration was quantitative but not qualitative (Fujise *et al.*, 1995). It is likely that the decrease of the transporter protein is a co-translational or posttranslational event that occurs simultaneously with or immediately after synthesis

and transfer of the protein to the plasma membrane, or due to an anomaly in gene expression. This is because amplification of the GLAST cDNA fragment was observed in normal reticulocytes as well as in bone marrow cells (Chapter 2, Fig. 12), while no noticeable Na^+-dependent uptake of glutamate was detected in reticulocytes obtained from LGluT dog S-1 made anemic by successive bleeding (data not shown).

The present study provided evidence indicating that the LGluT phenotype resulted from a complicated heterologous combination of several different alleles with mutations, being compatible with the prediction described above. First, we demonstrated that the GLAST protein with G492S mutation, which was the only causative mutation found in GLAST cDNA isolated from LGluT dogs, was unstable in the *Xenopus* oocyte expression system, while it was fully functional in terms of glutamate transport (Fig. 19). The instability of G492S GLAST would result in an aberrant deficiency of the transporter protein if G492S RNA serves as the major part of the GLAST gene transcript as observed in dogs II-1 and S-2 (Fig. 14). According to the proposed membrane topology of the human GLAST protein, Gly492 resides within the well-conserved intracellular C-terminal region (Seal and Amara, 1998) or in the 10th membrane-spanning β-sheet structure (Wahle and Stoffel, 1996). Alteration of this amino acid residue might affect the stability of the protein. In this respect, recent reports on phosphorylation-regulated ubiquitination of two proteins, IκBα (Chen *et al.*, 1995) and β-catenin (Orford *et al.*, 1997) are interesting. These studies demonstrated that phosphorylation of a specific Ser residue within the conserved target sequence led to ubiquitination and degradation of members of the IκBα and β-catenin families (Orford *et al.*, 1997), and this ubiquitination target sequence consisted of a motif of Asp-Ser-Gly-hydrophobic residue-any residue-Ser, similar to the mutant sequence surrounding the G492S locus, Asp-Ser-Leu-Gly-Ala-Ser492.

Second, a quantitative decrease of mRNA derived from the normal allele, which was observed in LGluT dogs heterozygous for G492S mutation, appeared to be an

additional cause of the reduced accumulation of total GLAST mRNA (Fig. 18). The decreased level of mRNA in these animals (I-1 and I-2), in combination with the instability of GLAST with G492S mutation, would lead to a defect of the transporter protein. Two types of GLAST cDNA were obtained from NGluT and LGluT dogs carrying G492S mutation in the heterozygous state (Fig. 14), and these cDNAs were basically identical except for the G492S mutation. Neither alternative splicing products nor additional mutations that might result in instability of the transcripts were observed in PCR amplification of bone marrow cDNAs from these LGluT dogs using several distinct primer pairs encompassing 5'- and 3'-stretched ends (data not shown). Therefore, some transcriptional regulation may be responsible for the selective reduction of normal GLAST mRNA.

Thus, the G492S mutation and its heterologous combination with some putative transcriptional defect as causes for GLAST protein deficiency appear to fit the appearance of the LGluT phenotype in the pedigree currently studied well. That is, dogs homozygous for G492S mutation, and also those heterozygous for G492S mutation and a selective decrease of normal GLAST mRNA, possess LGluT red cells in which the protein content and transport activity of GLAST are reduced to much less than 50% of those in NGluT dogs (Figs. 14, 17, and 18). The heterozygous existence of normal GLAST mRNA at a level even with that of G492S mutation seems to be sufficient to compensate for the GLAST protein and transport activity, resulting in the NGluT phenotype (dogs I-3 and III-4, Figs. 14 and 17).

Transcriptional regulation of GLAST appears to be responsible to the promoter sequence with housekeeping genes (Hagiwara *et al.*, 1996) as described in the previous Chapter. These findings raise intriguing questions as to whether the GLAST protein level, and therefore the transport activity in the central nervous system and the retinal cells of LGluT dogs, is affected as in erythroid cells and, if so, whether it causes neuronal or retinal dysfunction. Although these LGluT dogs have not exhibited serious

manifestations due to neuronal disorders, careful follow-up studies will provide information concerning these queries because chronic impairment of glutamate transport induces slow neurotoxicity (Rothstein *et al.*, 1993), and slight motor discoordination is the major sign observed in GLAST-knockout mice (Watase *et al.*, 1998). Analysis of the promoter regions of the GLAST gene is in progress.

It should be noted that red cells from HK dogs with LGluT phenotype had the mean corpuscular volume which was similar to that of LK dogs, while NGluT/HK dogs possessed overhydrated red cells with undefined etiologies (Table 3, and Maede *et al.*, 1982). Glutamate is accumulated in HK dog red cells at > 10 mM (Maede *et al.*, 1983). Decreased uptake of glutamate might reduce accumulation of glutamate, an anionic amino acid, which lead to entry of excess water into the cells, thus preventing overhydration. An alternate explanation would be possible. Recent studies have shown that application of substrates to the glutamate transporters elicits a chloride conductance that is thermodynamically uncoupled from substrate movement (Wadiche *et al.*, 1995; Seal and Amara, 1998), indicating that glutamate transporters including GLAST mediates both transport and chloride channel activity. Therefore, an alternate explanation would be possible that ion channel activity of GLAST somehow affect cell volume regulation of canine red cells.

In conclusion, this study identified GLAST in peripheral cells and its genetic variations in dogs. Studies on these animals should provide new insights into the structural and functional characterization and pathological implications of GLAST, a major glutamate transporter isoform.

General Conclusion

High-affinity Na^+-dependent glutamate transporters play important physiological roles in various mammalian tissues and cells. Several distinct glutamate transporters, GLAST, GLT-1, EAAC1, EAAT4, and EAAT5 have been cloned to date. In the central nervous system, these transporters are highly differentially localized and participate in glutamate uptake into glial or neuronal cells to terminate excitatory neurotransmission. They also participate in maintaining the extracellular glutamate concentration at the submicromolar level, thereby preventing accumulation of glutamate in the synaptic cleft, which causes overstimulation of the receptors and neurodegeneration. Dysfunction of glutamate transporters, therefore, has been considered to be involved in the pathogenesis of neurodegenerative diseases. In peripheral tissues, glutamate transporters are believed to have pivotal functions in epithelial transport and absorption of acidic amino acids, and in modulation of glutathione synthesis. However, physiological and pathological functions of other transporter isoforms in peripheral tissues have not been well characterized.

Canine red cells possess a high affinity Na^+- and K^+-dependent L-glutamate and L-aspartate transport system, despite the fact that most mammalian red cells are impermeable to these amino acids. Whereas dogs usually have red cells with low K^+ and high Na^+ concentrations (LK red cells), some Japanese Shiba and mongrel dogs have HK red cells with high K^+ and low Na^+ concentrations. HK red cells show accelerated Na^+/K^+-dependent glutamate uptake, leading to marked accumulations of intracellular glutamate, and reduced glutathione. Interestingly, these breeds also include dogs characterized by reduced or nondetectable red cell glutamate transport, generating variant HK cells without accumulation of glutathione. Such a hereditary defect of the glutamate transporter in mammals has never been described.

The long-range goal of the current study is to define the molecular basis that underlies the transport deficiency in canine red cells and facilitate our understanding of the regulatory mechanisms for expression of, and the physiological and pathological roles for, the glutamate transporter in various tissues, including the brain.

Chapter 1. Characterization of Na^+-dependent glutamate transport in canine red cells

In Chapter 1, stoichiometric and pharmacologic properties of Na^+-dependent L-glutamate transport in canine red cells were studied by using intact cells and resealed ghosts. The glutamate transport showed a precise dependence on extracellular Na^+ and intracellular K^+. Kinetical analysis revealed that two Na^+ ions and one K^+ ion were involved in each glutamate transport cycle. The glutamate transport was inhibited most potently by *threo*-3-hydroxyaspartate and L-cysteinesulfinate, and weakly by dihydrokainate and DL-α-aminoadipate, while no significant inhibition was observed for L-cysteine. Glutamate uptake was increased by internal, but not external, HCO_3^- when the internal and external anions of the red cell were replaced by several other anions. Moreover, this enhancement was blocked by inhibition of carbonic anhydrase, which indicated that glutamate transport was at least partly dependent on HCO_3^- generated inside the cells. These observations indicated that anion countertransport is coupled to the high-affinity Na^+/K^+-dependent glutamate transport in canine red cells. These stoichiometrical and pharmacological properties indicated that the glutamate transporter in canine red cells was a product of the glutamate transporter gene family and resembled a glial transporter GLAST.

Chapter 2. Identification of canine red cell Na^+-dependent glutamate transporter

Chapter 2 consisted of PCR-based cloning of cDNAs for four different canine brain glutamate transporters, functional analysis of the isolated clones in *Xenopus*

oocyte expression system, analysis on tissue distributions of the transcripts of transporter subtypes, and immunological identification of canine red cell transporter.

Canine GLAST, GLT-1, EAAC1, and EAAT4 cDNAs were isolated from brain cortex cDNAs by 5'- and 3'-RACE reactions. These transporters exhibited high-affinity Na^+-dependent glutamate transport (K_m values for glutamate were 23-56 μM) in *Xenopus* oocyte expression system except that EAAT4 did not show the transport activity. The oocytes microinjected with GLAST RNAs showed responses to the structural analogues of glutamate which were most consistent with those of glutamate transport in red cells. RT-PCR revealed strong signals for four different transporters in the brain and ubiquitous expression of GLAST. GLAST but not other subtypes showed amplification of cDNA fragments in bone marrow cells and reticulocytes. The GLAST cDNA that was 3.8 kb in length identical with that in the brain was isolated from bone marrow cDNAs. These results suggested that the GLAST protein functions in canine erythroid cells.

Immunoblotting analysis demonstrated the presence of 66-kDa glycoprotein in canine red cell membranes that was immunospecifically recognized with antibodies to synthetic C-terminal peptides of GLAST. Red cell GLAST was larger than that in the brain (60-62 kDa) due to a difference in N-linked oligosaccharides, and spontaneously formed dimers upon solubilization, being compatible with previous findings on brain glutamate transporters. These findings demonstrated that canine red cell glutamate transporter was the canine homologue of GLAST.

Chapter 3. Molecular basis for inherited defects of Na^+-dependent glutamate transport mediated by GLAST in canine red cells

Molecular basis for the inherited defects of the transport found in a family of dogs that led to decreased level of red cell glutathione and a high susceptibility to oxidative stress of red cells was investigated in Chapter 3.

Variant dog red cells, LGluT red cells characterized by an inherited remarkable decrease in glutamate transport activity showed decreased levels of reduced glutathione and were highly susceptible to oxidation. The GLAST protein content was extremely reduced in LGluT red cell membranes. All LGluT dogs carried a missense mutation of Gly492 to Ser (G492S) in either the heterozygous or homozygous state. The GLAST protein with G492S mutation was fully functional in glutamate transport in *Xenopus* oocytes. However, G492S GLAST exhibited a marked decrease in activity after the addition of cycloheximide, while the wild type showed no significant change, indicating that G492S GLAST was unstable compared to the wild-type transporter. Moreover, LGluT, but not normal, dogs heterozygous for G492S mutation showed a selective decrease in the accumulation of GLAST mRNA from the normal allele. Based on these findings, it was concluded that a complicated heterologous combination of G492S mutation and some transcriptional defect contributes to the pathogenesis of the LGluT red cell phenotype. Exact mechanisms for abnormal transcription and putative implications of defective glutamate transport in neurodegeneration remain to be determined.

In conclusion, the present study unequivocally demonstrated that canine red cell glutamate transporter was the canine homologue of GLAST, and showed the molecular basis for an inherited defect of red cell glutamate transport found in Japanese dogs.

Abstract

Canine red blood cells have a high-affinity Na^+/K^+-dependent glutamate transporter. In the present study, it is demonstrated that this transport is mediated by the canine homologue of GLAST, one of the glutamate transporter subtypes abundant in the central nervous system, based on the findings from PCR-based cDNA cloning and expression analyses of the brain and red cell transporters and immunological identification. It is also demonstrated that GLAST is the most ubiquitous glutamate transporter among the transporter subtypes that have been cloned to date. Canine red cell GLAST was a 66-kDa glycoprotein, slightly larger than that in the brain (60 kDa) due to the different *N*-glycosylation. The GLAST protein content was extremely reduced in variant red cells, LGluT red cells characterized by an inherited remarkable decrease in glutamate transport activity. Sequencing and expression analyses of the GLAST cDNAs from LGluT dogs demonstrated that a complicated heterologous combination of a missense mutation of Gly492 to Ser and some transcriptional defect contributes to pathogenesis of the LGluT red cell phenotype.

Acknowledgments

Dr. Yoshimitsu Maede (Hokkaido University) is gratefully appreciated for his helpful suggestions and critical review of the manuscript. The author gratefully appreciates Dr. Mutsumi Inaba (University of Tokyo) for his enthusiastic advises and suggestions on the present study and critical reading of the manuscript. The author thank Dr. Yoshiaki Habara, Dr. Mikinori Kuwabara and Dr, Shigeo Ito (Hokkaido University) for their critical reading of the manuscript and Dr. Katsumoto Kagota and Dr. Yoshiaki Hikasa (Tottori University) for their contribution to this study, Drs. Yuichi Takakuwa, and Eiko Ito (Tokyo Women's Medical University) for preparing of synthetic peptide, and Drs. Yuki Suwa, Aya Matsuu, Yukiko Futaoka, Kyoko Baba (Tottori University), Daishi Saito, Ichiro Koshino, and Mitsuhito Matsumoto (University of Tokyo) for their technical assistance.

References

Arriza, J. L., Eliasof, S., Kavanaugh, M. P., and Amara, S. G. (1997). Excitatory amino acid transporter 5, a retinal glutamate transporter coupled to a chloride conductance. *Proc. Natl. Acad. Sci. U. S. A.* **94**, 4155-4160.

Arizza, J. L., Fairman, W. A., Wadiche, J. I., Murdoch, G. H., Kavanaugh, M. P., and Amara, S. G. (1994). Functional comparisons of three glutamate transporter subtypes cloned from human motor cortex. *J. Neurosci.* **14**, 5559-5569.

Barbour, B., Brew, H., and Attwell, D. (1988). Electrogenic glutamate uptake in glial cells is activated by intracellular potassium. *Nature* **335**, 433-435.

Bouvier, M., Szatkowski, M., Amato, A., and Attwell, D. (1992). The glial cell glutamate uptake carrier countertransports pH-changing anions. *Nature* **360**, 471-474.

Bradford, M. M. (1976). A rapid and sensitive method for the quantitation of microgram quantities of protein utilizing the principle of protein-dye binding. *Anal. Biochem.* **72**, 248-254.

Cabantchik, Z. I., Knauf, P. A., and Rothstein, A. (1978). The anion transport system of the red blood cell. The role of membrane protein evaluated by the use of 'probes'. *Biochim. Biophys. Acta* **515**, 239-302.

Chaudhry, F. A., Lehre, K. P., van Lookeren Campagne, M., Ottersen, O. P., Danbolt, N. C., and Storm-Mathisen, J. (1995). Glutamate transporters in glial plasma membranes: highly differentiated localizations revealed by quantitative ultrastructural immunocytochemistry. *Neuron* **15**, 711-720.

Chen, Z., Hagler, J., Palombella, V. J., Melandri, F., Scherer, D., Ballard, D., and Maniatis, T. (1995). Signal-induced site-specific phosphorylation targets IκBα to the ubiquitin-proteasome pathway. *Genes Dev.* **9**, 1586-1597.

Deneke, S. M., Steiger, V., and Fanburg, B. L. (1987). Effect of hyperoxia on glutathione levels and glutamic acid uptake in endothelial cells. *J. Appl. Physiol.*

63, 1966-1971.

Fairman, W. A., Vandenberg, R. J., Arriza, J. L., Kavanaugh, M. P., and Amara, S. G. (1995). An excitatory amino-acid transporter with properties of a ligand-gated chloride channel. *Nature* **375**, 599-603.

Fujise, H., Hamada, Y., Mori, M., and Ochiai, H. (1995). Na-dependent glutamate transport in high K and high glutathione (HK/HG) and high K and low glutathione (HK/LG) dog red blood cells. *Biochim. Biophys. Acta* **1239**, 22-26.

Fujise, H., Mori, M., Ogawa, E., and Maede, Y. (1993). Variant of canine erythrocytes with high potassium content and lack of glutathione accumulation. *Am. J. Vet. Res.* **54**, 602-606.

Grone, A., Weckmann, M. T., Capen, C. C., and Rosol, T. J. (1996). Canine glyceraldehyde-3-phosphate dehydrogenase complementary DNA: polymerase chain reaction amplification, cloning, partial sequence analysis, and use as loading control in ribonuclease protection assays. *Am. J. Vet. Res.* **57**, 254-257.

Hagiwara, T., Tanaka, K., Takai, S., Maeno-Hikichi, Y., Mukainaka, Y., and Wada, K. (1996). Genomic organization, promoter analysis, and chromosomal localization of the gene for the mouse glial high-affinity glutamate transporter Slc1a3. *Genomics* **33** , 508-515.

Harada, T., Harada, C., Watanabe, M., Inoue, Y., Sakagawa, T., Nakayama, N., Sasaki, S., Okuyama, S., Watase, K., Wada, K., and Tanaka, K. (1998). Functions of the two glutamate transporters GLAST and GLT-1 in the retina. *Proc. Natl. Acad. Sci. U. S. A.* **95** , 4663-4666.

Haugeto, O., Ullensvang, K., Levy, L. M., Chaudhry, F. A., Honore, T., Nielsen, M., Lehre, K. P., and Danbolt, N. C. (1996). Brain glutamate transporter proteins form homomultimers. *J. Biol. Chem.* **271** , 27715-27722.

Heinz, E., Sommerfeld, D. L., and Kinne, R. K. (1988). Electrogenicity of sodium/L-glutamate cotransport in rabbit renal brush-border membranes: a reevaluation. *Biochim. Biophys. Acta.* **937** , 300-308.

Hoeltzli, S. D., Kelley, L. K., Moe, A. J., and Smith, C. H. (1990). Anionic amino acid transport systems in isolated basal plasma membrane of human placenta. *Am. J. Physiol.* **259** , C47-C55.

Inaba, M., and Maede, Y. (1984). Increase of Na^+ gradient-dependent L-glutamate and L-aspartate transport in high K^+ dog erythrocytes associated with high activity of (Na^+, K^+)-ATPase. *J. Biol. Chem.* **259** , 312-317.

Inaba, M., and Maede, Y. (1986). Na,K-ATPase in dog red cells. Immunological identification and maturation-associated degradation by the proteolytic system. *J. Biol. Chem.* **261** , 16099-16105.

Inaba, M., Yawata, A., Koshino, I., Sato, K., Takeuchi, M., Takakuwa, Y., Manno, S., Yawata, Y., Kanzaki, A., Sakai, J., Ban, A., Ono, K., and Maede, Y. (1996). Defective anion transport and marked spherocytosis with membrane instability caused by hereditary total deficiency of red cell band 3 in cattle due to a nonsense mutation. *J. Clin. Invest.* **97** , 1804-1817.

Inoue, K., Sakaitani, M., Shimada, S., and Tohyama, M. (1995). Cloning and expression of a bovine glutamate transporter. *Mol. Brain Res.* **28**, 343-348.

Kanai, Y. (1997). Family of neutral and acidic amino acid transporters: molecular biology, physiology and medical implication. *Curr. Opin. Cell Biol.* **9**, 565-572.

Kanai, Y., and Hediger, M. A. (1992). Primary structure and functional characterization of a high-affinity glutamate transporter. *Nature* **360**, 467-471.

Kanner, B. I. (1978). Active transport of γ-aminobutyric acid by membrane vesicles isolated from rat brain. *Biochemistry* **17**, 1207-1211.

Kanner, B. I., Danbolt, N., Pines, G., Koepsell, H., Seeberg, E., and Storm-Mathisen, J. (1993). Structure and function of the sodium and potassium-coupled glutamate transporter from rat brain. *Biochem. Soc. Trans.* **21**, 59-61.

Kanner, B. I., and Sharon, I. (1978). Active transport of L-glutamate by membrane vesicles isolated from rat brain. *Biochemistry* **17**, 3949-3953.

Kawakami, H., Tanaka, K., Nakayama, T., Inoue, K., and Nakamura, S. (1994). Cloning and expression of a human glutamate transporter. *Biochem. Biophys. Res. Commun.* **199**, 171-176.

Klonk, S., and Deuticke, B. (1992). Involvement of cytoskeletal proteins in the barrier function of the human erythrocyte membrane. I. Impairment of resealing and formation of aqueous pores in the ghost membrane after modification of SH groups. *Biochim. Biophys. Acta* **1106** , 126-136.

Lehre, K. P., Levy, L. M., Ottersen, O. P., Storm-Mathisen, J., and Danbolt, N. C. (1995). Differential expression of two glial glutamate transporters in the rat brain: quantitative and immunocytochemical observations. *J. Neurosci.* **15** , 1835-1853.

Lin, C. L., Bristol, L. A., Jin, L., Dykes-Hoberg, M., Crawford, T., Clawson, L., and Rothstein, J. D. (1998). Aberrant RNA processing in a neurodegenerative disease: the cause for absent EAAT2, a glutamate transporter, in amyotrophic lateral sclerosis. *Neuron* **20** , 589-602.

Maede, Y., and Inaba, M. (1985). (Na,K)-ATPase and Ouabain binding in reticulocytes from dogs with high K and low K erythrocytes and their changes during maturation. *J. Biol. Chem.* **260** , 3337-3343.

Maede, Y., Inaba, M., and Taniguchi, N. (1983). Increase of Na-K-ATPase activity, glutamate, and aspartate uptake in dog erythrocytes associated with hereditary high accumulation of GSH, glutamate, glutamine, and aspartate. *Blood* **61** , 493-499.

Maede, Y., Kasai, N., and Taniguchi, N. (1982). Hereditary high concentration of glutathione in canine erythrocytes associated with high accumulation of glutamate, glutamine, and aspartate. *Blood* **59**, 883-889.

Maede, Y., Kuwabara, M., Sasaki, A., Inaba, M., and Hiraoka, W. (1989). Elevated glutathione accelerates oxidative damage to erythrocytes produced by aromatic

disulfide. *Blood* **73**, 312-317.

Nicholls, D., and Attwell, D. (1990). The release and uptake of excitatory amino acids. *Trends Pharmacol. Sci*. **11**, 462-468.

Orford, K., Crockett, C., Jensen, J. P., Weissman, A. M., and Byers, S. W. (1997). Serine phosphorylation-regulated ubiquitination and degradation of β-catenin. *J. Biol. Chem*. **272**, 24735-8.

Payne, J. A., Lytle, C., and McManus, T. J. (1990). Foreign anion substitution for chloride in human red blood cells: effect on ionic and osmotic equilibria. *Am. J. Physiol.* **259**, C819-C827.

Pines, G., Danbolt, N. C., Bjoras, M., Zhang, Y., Bendahan, A., Eide, L., Koepsell, H., Storm-Mathisen, J., Seeberg, E., and Kanner, B. I. (1992). Cloning and expression of a rat brain L-glutamate transporter. *Nature* **360**, 464-467.

Rajendran, V. M., Harig, J. M., Adams, M. B., and Ramaswamy, K. (1987). Transport of acidic amino acids by human jejunal brush-border membrane vesicles. *Am. J. Physiol.* **252**, G33-G39.

Recasens, M., Varga, V., Nanopoulos, D., Saadoun, F., Vincendon, G., and Benavides, J. (1982). Evidence for cysteine sulfinate as a neurotransmitter. *Brain Res.* **239**, 153-173.

Roskoski, R., Jr., Rauch, N., and Roskoski, L. M. (1981). Glutamate, aspartate, and γ-aminobutyrate transport by membrane vesicles prepared from rat brain. *Arch. Biochem. Biophys*. **207**, 407-415.

Rothstein, J. D., Dykes-Hoberg, M., Pardo, C. A., Bristol, L. A., Jin, L., Kuncl, R. W., Kanai, Y., Hediger, M. A., Wang, Y., Schielke, J. P., and Welty, D. F. (1996). Knockout of glutamate transporters reveals a major role for astroglial transport in excitotoxicity and clearance of glutamate. *Neuron* **16**, 675-686.

Rothstein, J. D., Jin, L., Dykes-Hoberg, M., and Kuncl, R. W. (1993). Chronic

inhibition of glutamate uptake produces a model of slow neurotoxicity. *Proc. Natl. Acad. Sci. U. S. A.* **90**, 6591-6595.

Sato, K., Inaba, M., and Maede, Y. (1994). Characterization of Na^+-dependent L-glutamate transport in canine erythrocytes. *Biochim. Biophys. Acta* **1195**, 211-217.

Schlag, B. D., Vondrasek, J. R., Munir, M., Kalandadze, A., Zelenaia, O. A., Rothstein, J. D., and Robinson, M. B. (1998). Regulation of the glial Na^+-dependent glutamate transporters by cyclic AMP analogs and neurons. *Mol. Pharmacol.* **53**, 355-369.

Schneider, E. G., Hammerman, M. R., and Sactor, B. (1980). Sodium gradient-dependent L-glutamate transport in renal brush border membrane vesicles. *J. Biol. Chem.* **255**, 7650-7656.

Seal, R. P., and Amara, S. G. (1998). A reentrant loop domain in the glutamate carrier EAAT1 participates in substrate binding and translocation. *Neuron* **21**, 1487-1498.

Sips, H. J., de Graaf, P. A., and van Dam, K. (1982). Transport of L-aspartate and L-glutamate in plasma-membrane vesicles from rat liver. *Eur. J. Biochem.* **122**, 259-64.

Storck, T., Schulte, S., Hofmann, K., and Stoffel, W. (1992). Structure, expression, and functional analysis of a Na^+-dependent glutamate/aspartate transporter from rat brain. *Proc. Natl. Acad. Sci. U. S. A.* **89**, 10955-10959.

Szatkowski, M., and Attwell, D. (1994). Triggering and execution of neuronal death in brain ischaemia: two phases of glutamate release by different mechanisms. *Trends. Neurosci.* **17**, 359-365.

Tanaka, K. (1993). Expression cloning of a rat glutamate transporter. *Neurosci. Res.* **16**, 149-153.

Tanaka, K., Watase, K., Manabe, T., Yamada, K., Watanabe, M., Takahashi, K., Iwama, H., Nishikawa, T., Ichihara, N., Kikuchi, T., Okuyama, S., Kawashima, N., Hori, S., Takimoto, M., and Wada, K. (1997). Epilepsy and exacerbation of brain injury in mice lacking the glutamate transporter GLT-1. *Science* **276**, 1699-1702.

Trotti, D., Danbolt, N. C., and Volterra, A. (1998). Glutamate transporters are oxidant-vulnerable: a molecular link between oxidative and excitotoxic neurodegeneration? *Trends Pharmacol. Sci*. **19**, 328-334.

Trotti, D., Rolfs, A., Danbolt, N. C., Brown, R. H., Jr., and Hediger, M. A. (1999). SOD1 mutants linked to amyotrophic lateral sclerosis selectively inactivate a glial glutamate transporter. *Nat. Neurosci.* **2**, 427-433.

Wadiche, J. I., Amara, S. G., and Kavanaugh, M. P. (1995). Ion fluxes associated with excitatory amino acid transport. *Neuron* **15**, 721-728.

Wahle, S., and Stoffel, W. (1996). Membrane topology of the high-affinity L-glutamate transporter (GLAST-1) of the central nervous system. *J. Cell Biol.* **135**, 1867-1877.

Watase, K., Hashimoto, K., Kano, M., Yamada, K., Watanabe, M., Inoue, Y., Okuyama, S., Sakagawa, T., Ogawa, S., Kawashima, N., Hori, S., Takimoto, M., Wada, K., and Tanaka, K. (1998). Motor discoordination and increased susceptibility to cerebellar injury in GLAST mutant mice. *Eur. J. Neurosci.* **10**, 976-988.

Young, J. D., and Ellory, J. C. (1977). *In* Membrane Transport in Red Cells (Ellory, J. C., and Lew, V. L. eds.) (London: Academic Press), pp. 301-325.

Zerangue, N., and Kavanaugh, M. P. (1996). Interaction of L-cysteine with a human excitatory amino acid transporter. *J. Physiol.* **493**, 419-423.